การพัฒนาและวิเคราะห์คุณลักษณะของแผ่นนาโนคอมพอสิตจากแบคทีเรียเซลลูโลสและยางธรรมชาติ

นางสาวกรกมล โพธิวาระ

วิทยานิพนธ์นี้เป็นส่วนหนึ่งของการศึกษาตามหลักสูตรปริญญาวิศวกรรมศาสตรมหาบัณฑิต
สาขาวิชาวิศวกรรมเคมี ภาควิชาวิศวกรรมเคมี
คณะวิศวกรรมศาสตร์ จุฬาลงกรณ์มหาวิทยาลัย
ปีการศึกษา 2559

DEVELOPMENT AND CHARACTERIZATION OF BACTERIAL CELLULOSE/NATURAL RUBBER COMPOSITE FILMS

Miss Kornkamol Potivara

A Thesis Submitted in Partial Fulfillment of the Requirements
for the Degree of Master of Engineering Program in Chemical Engineering
Department of Chemical Engineering
Faculty of Engineering
Chulalongkorn University
Academic Year 2016

Thesis Title	DEVELOPMENT AND CHARACTERIZATION OF BACTERIAL CELLULOSE/NATURAL RUBBER COMPOSITE FILMS
By	Miss Kornkamol Potivara
Field of Study	Chemical Engineering
Thesis Advisor	Associate ProfessorMuenduen Phisalaphong, Ph.D.

Accepted by the Faculty of Engineering, Chulalongkorn University in Partial Fulfillment of the Requirements for the Master's Degree

.....Dean of the Faculty of Engineering
(Associate ProfessorSupot Teachavorasinskun, D.Eng.)

THESIS COMMITTEE

.....Chairman
(ProfessorBunjerd Jongsomjit, Ph.D.)

.....Thesis Advisor
(Associate ProfessorMuenduen Phisalaphong, Ph.D.)

.....Examiner
(ProfessorArtiwan Shotipruk, Ph.D.)

.....External Examiner
(Jeerun Kingkaew, D.Eng.)

กรกมล โพธิวาระ : การพัฒนาและวิเคราะห์คุณลักษณะของแผ่นนาโนคอมพอสิตจากแบคทีเรียเซลลูโลสและยางธรรมชาติ (DEVELOPMENT AND CHARACTERIZATION OF BACTERIAL CELLULOSE/NATURAL RUBBER COMPOSITE FILMS) อ.ที่ปรึกษาวิทยานิพนธ์หลัก: รศ. ดร. เหมือนเดือน พิศาลพงศ์, 101 หน้า.

งานวิจัยนี้เป็นการพัฒนาวัสดุคอมพอสิตจากแบคทีเรียเซลลูโลสและยางธรรมชาติ เพื่อปรับปรุงคุณสมบัติความยืดหยุ่นของแผ่นนาโนเซลลูโลสสามารถทำได้โดยการเติมยางธรรมชาติที่มีคุณสมบัติความยืดหยุ่นสูง โดยวิธีการนำแผ่นนาโนเซลลูโลสที่ได้จากการเลี้ยงเชื้อในสภาวะนิ่งไปแช่ในน้ำยางธรรมชาติที่ความเข้มข้น 0.5-10 เปอร์เซ็นต์ (ปริมาตร ต่อ ปริมาตร) และอุณหภูมิในการแช่ 30-70 องศาเซลเซียส โดยเติมเอทานอลเพื่อลดความหนืดของสารละลายเพิ่มการยึดติดของอนุภาคยางธรรมชาติ ผลจากการศึกษาถูกนำมาเปรียบเทียบกับแผ่นนาโนเซลลูโลสที่ไม่ผ่านกระบวนการแช่ การวิเคราะห์ขนาดอนุภาคน้ำยางที่ปรับปรุงด้วยเอทานอลถูกศึกษาด้วยเครื่องวัดขนาดอนุภาคโดยใช้เทคนิคการเลี้ยวเบนของแสง ในขณะที่แผ่นนาโนเซลลูโลสที่ปรับปรุงด้วยยางธรรมชาติจะถูกนำไปวิเคราะห์ลักษณะสัณฐานวิทยาและภาคตัดขวางด้วยเครื่องจุลทรรศน์อิเล็กตรอนแบบส่องกราด, หมู่ฟังก์ชันและแรงกระทำระหว่างโมเลกุลด้วยเครื่องเครื่องฟลูเรียร์ทรานส์ฟอร์ม อินฟราเรดสเปคโทรมิเตอร์, ความเป็นผลึกด้วยวิเคราะห์การเลี้ยวเบนรังสีเอกซ์, สมบัติทางความร้อนด้วยเครื่องดิฟเฟอเรนเชียล สแกนนิง แคลอริมิเตอร์, สมบัติเชิงกลด้วยเครื่องทดสอบแรงดึง ศึกษาการดูดซึมน้ำ, โทลูอีน รวมถึงการย่อยสลายของวัสดุคอมพอสิตในดิน จากผลการทดลองพบว่าการเติมเอทานอลทำให้ความหนืดของน้ำยางลดลงและส่งผลต่อการแพร่ของอนุภาคยางเข้าในแผ่นแบคทีเรียเซลลูโลสได้ดีขึ้น สภาวะที่เหมาะสมที่ทำให้ยางธรรมชาติสามารถยึดติดบนแผ่นนาโนเซลลูโลสได้ดี คือ ความเข้มข้นของยางธรรมชาติเป็น 2.5 และ 5 เปอร์เซ็น ที่อุณหภูมิในการแช่เป็น 50 และ 60 องศาเซลเซียส ส่งผลให้มีความหนาของวัสดุคอมพอสิตเพิ่มสูงขึ้นจากแผ่นแบคทีเรียเซลลูโลสที่ไม่ได้ปรับปรุงความหนา 12 ไมโครเมตร เป็น 20-27 ไมโครเมตร จากการวิเคราะห์คุณสมบัติความเป็นผลึกและแรงกระทำระหว่างโมเลกุลของวัสดุคอมพอสิตระหว่างนาโนเซลลูโลสและยางธรรมชาติพบว่า ยางธรรมชาติไม่ได้เกิดอันตรกิริยาทางเคมีกับแผ่นนาโนเซลลูโลสและไม่ทำให้คุณสมบัติความเป็นผลึกของแผ่นนาโนเซลลูโลสเปลี่ยนไป แต่อย่างไรก็ตามการเติมยางธรรมชาติบนแผ่นนาโนเซลลูโลสทำให้ความสามารถในการดูดน้ำของแผ่นนาโนเซลลูโลสลดลง และความสามารถในการดูดซับโทลูอีนเพิ่มขึ้น นอกจากนี้ยังสามารถปรับปรุงคุณสมบัติเชิงกลของแผ่นนาโนเซลลูโลสได้โดยเพิ่มความสามารถในการต้านทานต่อแรงดึงและค่าเปอร์เซ็นต์การดึงยืดของวัสดุที่เพิ่มมากขึ้น โดยมีค่าสูงขึ้น 3-6 เท่าเปรียบเทียบกับแผ่นแบคทีเรียเซลลูโลสที่ไม่ได้ปรับปรุง และวัสดุคอมพอสิตสามารถย่อยสลายได้อย่างสมบูรณ์ภายใน 5-6 สัปดาห์

ภาควิชา วิศวกรรมเคมี ลายมือชื่อนิสิต .....

สาขาวิชา วิศวกรรมเคมี ลายมือชื่อ อ.ที่ปรึกษาหลัก .....

ปีการศึกษา 2559

5770105821 : MAJOR CHEMICAL ENGINEERING

KEYWORDS: BACTERIAL CELLULOSE / NATURAL RUBBER / IMMERSION PROCESS

KORNKAMOL POTIVARA: DEVELOPMENT AND CHARACTERIZATION OF BACTERIAL CELLULOSE/NATURAL RUBBER COMPOSITE FILMS. ADVISOR: ASSOC. PROF.MUENDUEN PHISALAPHONG, Ph.D., 101 pp.

The composite of bacterial cellulose (BC) and natural rubber (NR) has been developed in this study to combine the prominent properties between strength from three-dimensional structure of BC nanocellulose and flexible molecular chain of isoprene (C_5H_8). BC membranes were produced by *A. xylinum* using coconut-water medium under static incubation for 5 days. The BC membrane were then purified and immersed in NR latex solution at various concentrations (0-10 % v/v). The influence immersion temperature (30℃, 50℃, 60℃ and 70℃) and a ratio of ethanol in the solvent were also investigated. The results were compared with the unmodified BC. NR particles were characterized by Laser particle size distribution (PSD), the morphology and cross-section of films by Field Emission Scanning Electron Microscopy (FESEM), functional groups and intermolecular interactions by Fourier Transform Infrared Spectroscopy (FTIR), the crystallinity structure by X-ray diffraction (XRD), the thermal properties of composite films by Differential Scanning Calorimetry (DSC), the mechanical properties by Instron testing machine, the water absorption capacity, toluene uptake and biodegradable in soil measurements. According to the experiments, the addition of a certain amount of ethanol slightly affected NR particle size but helped reduce the viscosity of NRL, resulting in more penetration of NR molecules into BC. The optimal condition was the immersion at 2.5–5.0 % NR latex solution, under the temperature of 50-60℃, where the thickness of the composite could be enhanced from ~12 μm of the unmodified BC to ~20-27 μm. The crystallinity structure of the composite films remained as BC structure. The new peak was not occurred from FTIR analysis; however a slight shift of hydroxyl peaks might indicate some weak physical interactions between BC and NR. The results show that the water absorption decreased and the toluene uptake increased as compared to normal BC film. Moreover, the tensile strength and elongation at break of the NR-BC composited films were significantly improved for 3-6 folds in comparison to the normal BC film. The results of biodrgradation in soil showed that the composite films could completely degrade for 5-6 weeks.

Department: Chemical Engineering Student's Signature .....

Field of Study: Chemical Engineering Advisor's Signature .....

Academic Year: 2016

ACKNOWLEDGEMENTS

First of all, I would like to express my gratitude and appreciation to my advisor, Associate Professor Dr.Muenduen Phisalaphong, my advisor, for her best suggestion, useful discussion and knowledge for this research.

This work was supported by the Ratchadaphiseksomphot Endowment Funds, Chulalongkorn University of project CU-58-032-AM and the Institutional Research Grant (The Thailand Research Fund), IRG5780014, and Chulalongkorn University, Contract No.RES_57_411_21_076

The author would also be grateful to Professor Dr. Bunjerd Jongsomjit, as the chairman, Professor Dr.Artiwan Shotipruk and Dr.Jeerun Kingkaew, as the members of the thesis committee.

Furthermore, the author would like to be thanks for kind suggestions and useful help from all student member of Associate Professor Muenduen groups as well as my friends in the lab of Chemical Engineering Research Unit for value Adding of Bioresources.

Finally, she would like to dedicate the achievement of this work to her parents, who have always been the source of her suggestion, support and encouragement.

CONTENTS

Page

Page

Page

TABLE CONTENTS

Page

FIGURE CONTENTS

Page

CHAPTER 1
INTRODUCTION

1.1 Motivation

Bacterial cellulose (BC) is a product from the nature which can be produced by many species of bacteria such as *Acetobactor (Gluconacetobactor), Agrobacterium, Achromebactor, Aerobactor, Azotobactor, Rhizobium, Sarcina, Salmonella* and *Escherichia*. However, *Acetobactor* is the most wildly used bacteria the synthesis of BC. Special properties of BC include high purity (excluding hemicellulose and lignin), high crystallinity and Young's modulus, excellent biodegradability, large water holding capacity up to hundred times its weight, excellent biological affinity [1]. With many advantageous characteristics, BC has been supplied in many branches, for example, artificial skin for patient with burn ulcers [2], emulsion-stabilizing compound for paper industry [3], artificial blood vessels [4], drug delivery, tissue engineering [5], cardiovascular tissues [6], and artificial skin for wound healing [7].

Natural rubber latex (NRL) is a concentrated colloidal suspension produced by the rubber tree. NRL is mainly composed of isoprene (2-methyl1, 3-butadiene (Formula: C_5H_8; Molecular weight: 68). Natural rubber (NR) is a natural polymer of isoprene. It is a biodegradable material. The most important property of NR is elasticity, which is the ability to return to its original shape and size. However, some properties of NR may need to be adjusted, for example, hardness, young modulus, abrasion resistance [8]. Normally, fibers are used as reinforcement in NRL and then it is cross-linked with acid to improve bonding of composite materials. Various natural fibers have been used as a reinforcement in NR matrix, such as sisal/oil palm hybrid fiber [9], pineapple fiber [10], coconut fiber [11], bamboo fiber [12], and grass fiber [13].

According to the literature review, there are only few of researches of BC reinforced with NR. In order to obtain films with the mechanical property of combined materials between BC, which is characterized by high strength and hardness, and NR, which is characterized by high elasticity, in this study, NR-BC film is developed and characterized. A bacterial cellulose (BC) hydrogel is modified via impregnation by

diffusion of NRL and cross-linking with acetic acid solution. NR-BC films are then configured and characterized for chemical, physical/mechanical and biological properties.

1.2 Objectives

1.2.1 To synthesis BC and develop NR-BC composite films by immersion method.

1.2.2 To characterize the morphology, chemical, physical/mechanical and biological properties of NR-BC composite films.

1.3 Research scopes

1.3.1 Biosynthesis of BC hydrogel by *Acetobactor xylinum* (AGR60)

1.3.2 Modification of the BC film by immersing BC in NRL dispersion at 0-10% at 30, 50, 60, 70°C for 48 hours and find the optimum conditions.

1.3.3 Characterization of the NR-BC films by:

a. Field emission scanning electron microscopy (FESEM).

b. Laser particle size distribution (PSD)

c. Fourier transform infrared spectroscopy (FTIR)

d. The solvent uptake study of water and toluene

e. X-ray diffractometer (XRD)

f. Differential scanning calorimetry (DSC)

g. Thermal gravimetric analysis (TGA)

h. Universal testing machine (UTM)

f. Biodegradation in soil.

1.4 Overview

This present work was organized as follows:

- Chapter I presents an introduction of this study
- Chapter II contains background theory of bacterial cellulose, natural rubber and the literature review
- Chapter III states the details of the experimental procedures and techniques of this research
- Chapter IV reviews the experimental results of the characterization NR-BC Films.
- Chapter V contains the overall conclusion obtained from this research. Future works and recommendations are also stated.

Finally, the additional data of the experiments which had emerged from this study are included in appendixes at the end of this thesis.

CHAPTER 2

THEORY AND LITERATURE REVIEW

2.1 Cellulose from the plants

Cellulose, a linear polysaccharide, is an organic compound with the formula $(C_6H_{10}O_5)_n$ a linear chain consisting of β (1,4) linked D-glucose units about 15 - 40,000 units. The average molecular weight is depending on the type of cellulose. Plant celluloses are unpurified, mostly bond to other polymers in the cell wall of plants such as pectin, lignin, and hemicelluloses [14].

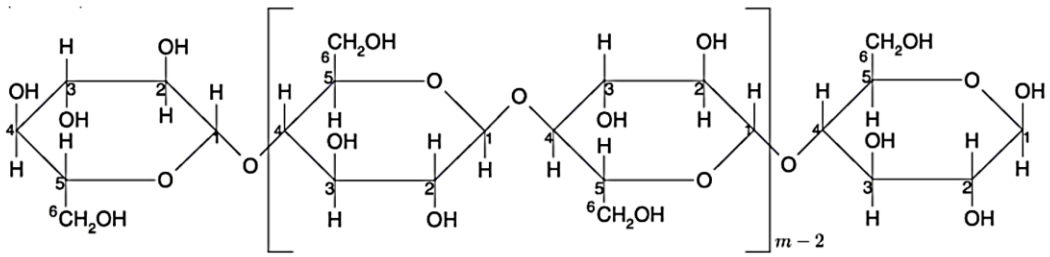

Figure 2. 1 The chemical structure of cellulose. The disaccharide, cellobiose, is the basic repeat unit and is enclosed in brackets.

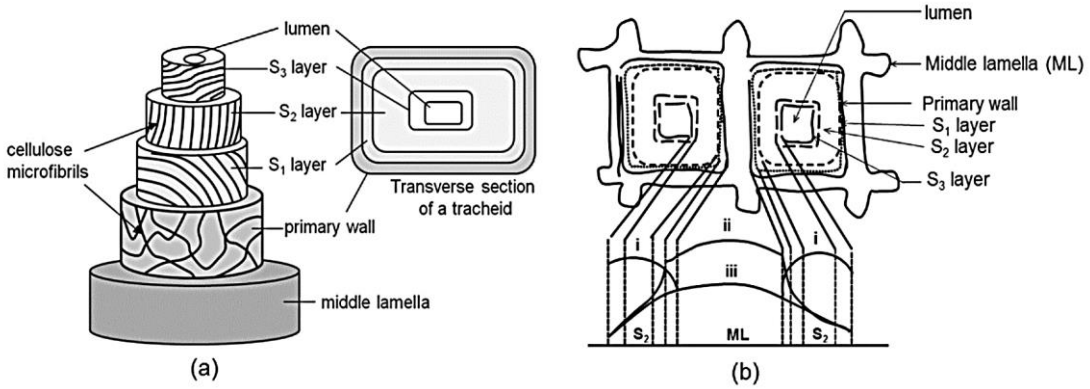

Figure 2. 2 (a) Three-dimensional structure of the secondary cell wall of a xylem cell and (b) the relative amounts of cellulose, hemicellulose, and lignin across a cross-section of two wood cells (i: cellulose; ii: lignin; and iii: hemicelluloses) [15].

2.2 Bacterial cellulose from *Acetobactor xylinum*.

2.2.1 Bacterial cellulose from various microorganism

Bacterial cellulose (BC) is a biomaterial which is well known in name of Nata de Coco, product from primary metabolism processes of microbes. The overview of bacterial cellulose procedure was shown in Table 2.1

Table 2. 1 Bacterial cellulose procedures [16].

Organisms(genus)	Cellulose produced	Biological role
Acetobactor	Extracellular pellicle Cellulose ribbons	To keep in aerobic environment
Aerobactor	Cellulose fibrils	Flocculation in waste water
Agrobacterium	Short cellulose	Attach to plant tissue
Alicaligenes	Cellulose fibrils	Flocculation in wastewater
Pseudomonas	No distinct fibrils	Flocculation in wastewater
Rhizobium	Short fibrils	Attached to most plant
Zoogloea	Not well defined	Flocculation in wastewater

Acetobactor xylinum is acetic acid bacteria, gram negative, rod shape, which oxidize sugars or ethanol. During the fermentation acetic acid and pure cellulose fiber will be produced. Pure cellulose fiber is not contaminated by hemicellulose, lignin and pectin and high hydrophilic surface area. BC can absorb water as high as 60-700 times on its dry weight. The diameters of BC nanocellulose fibers approximately 20-100 nanometers, which is smaller than the fibers of plants for 10-10,000 times and about 100 times smaller than the polyester fibers. BC has high mechanical strength [17-19] and its isotropic Young's modulus is about 20 GPa [20, 21] while isotropic Young's modulus of single fiber is about 130 GPa by Raman spectroscopy techniques[22, 23].

2.2.2 Biosynthesis of BC

The synthesis of cellulose in *Acetobactor xylinum* or any type of cellulose-producing organisms including plants are two steps to synthesis the first formation of with polymerization of glucose units and the second is assembly and crystallization of cellulose chain, the rate of polymerization is limited by the rate of assemble and crystallization [24]. The formation of cellulose fibrils is shown in Fig 2.3

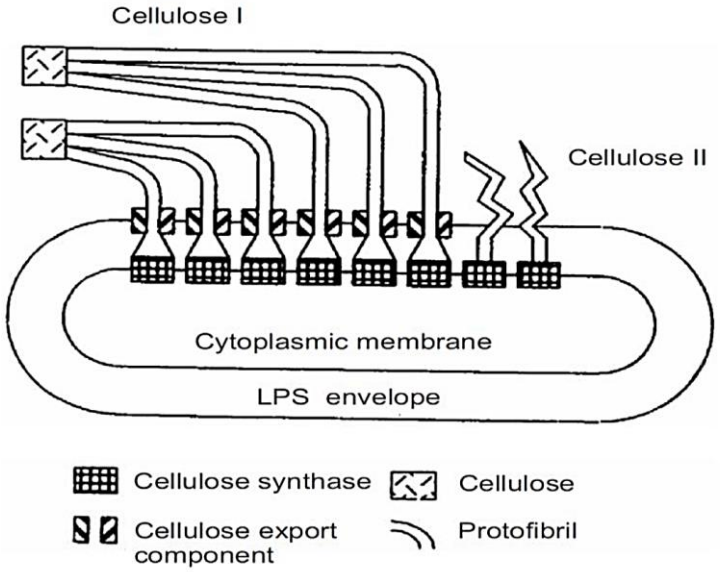

Figure 2. 3 Production of cellulose microfibrils by Acetobactor xylinum [24].

A. xylinum are able to convert various carbon compounds, for example glucose, fructose or hexoses into cellulose through a complex biological process. BC fiber from extrusion of chains and assembly outside the cells has unique structure and property. Initially cellulose molecules synthesized in the interior of bacterial cell and spun out of the cellulose export components[17]. The cellulose is occurred in the cytoplasmic membrane. The protofibrils have diameter 2-4 nm, ribbon-shaped microfibrils, dimension 80×4 by approximate [17, 24].

2.2.3 Bacterial cellulose synthesis

Synthesis of bacterial cellulose is a multi-step process, at least four step, involving with enzyme, catalyst and precursors. Pathways and mechanism of uridine diphosphoglucose (UDPGlc) can be simplify as showed in Fig 2.4

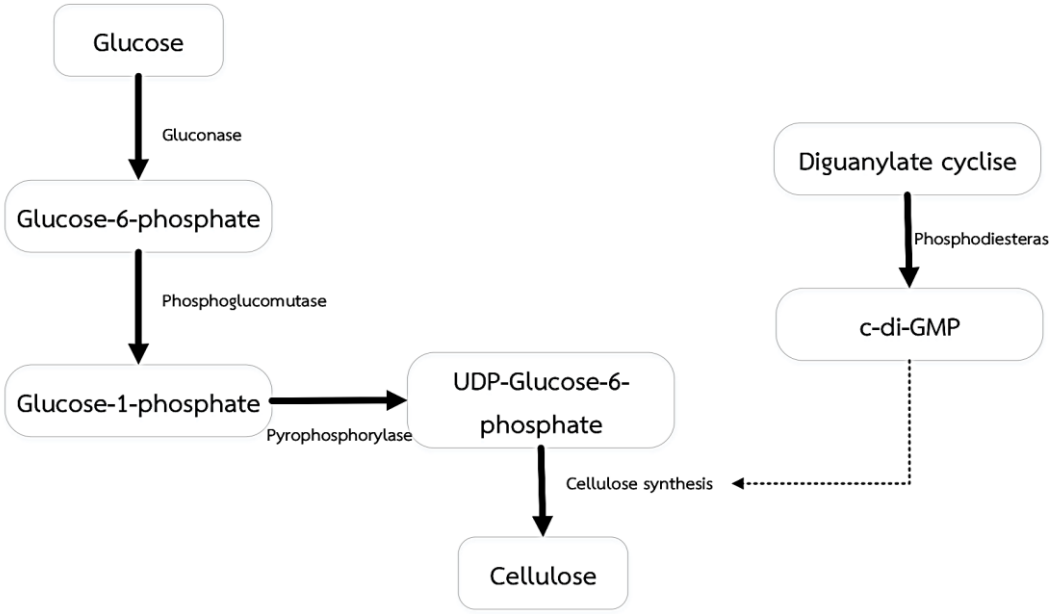

Figure 2. 4 Simplified pathways of carbon metabolism in *Acetobactor xylinum*. Reproduced with modifications from Ross et al. (1991) and [25].

The direct cellulose precursor is UDPGlc which is a product of conventional pathway and common in many organisms. Cellulose can be produced as follows; firstly, glucose or other carbon compound is converted into glucose-6-phosphate by the enzyme gluconosane and then isomerization of glucose-6-phosphate into glucose-1-phosphate by the enzyme phosphoglucomutase. After that, glucose-1-phosphate is converted into uridine diphosphate-glucose-6-phosphate (UDPGlc) by the enzyme pyrophosporylase. Cyclic nucleotide (c-di-GMP) is used for activate cell, which can be synthesized in *A. xylinum* by enzyme diguanylate cyclise and the concentration is controlled by the action of phosphodiesterases. Then UPDG is polymerized into cellulose by an enzyme called cellulose synthase [26].

The morphology of BC depends on the growing culture environment. Important food sources for fermentation are:

Carbon is the main component for energy of cellulose chain. Many materials can be used as carbon source. For example, coconut water, coconut milk, pineapple juice etc. Coconut water is widely used because it is a waste from the coconut milk industry. However, depending on the species of coconut, it is necessary to add sugar into it in order to have a sufficient amount of carbon for cellulose.

Nitrogen is another important component; 8-10 weight percent of cells is nitrogen. Protein in coconut water contains nitrogen, of about 0.4%. Therefore, nitrogen compounds should be added into the culture medium to accelerate the creation of pellicle to thicken in the short time. From studying, ammonium dihydrogen phosphate ($NH_4H_2PO_4$) of 0.5 percent can help produce BC pellicle higher than nitrogen from other sources, for example, ammonium sulphate $(NH_4)_2SO_4$, potassium nitrate (KNO_3), sodium nitrate ($NaNO_3$), yeast extract, corn steep liquor etc [27].

A. xylinum well grows in pH 3.5-7.5 and the optimum pH for the metabolism is 4.5 - 6.0 [28]. It was reported that the increase of acetic acid for 1% can protect contamination of *Aspergillus* sp. and the increase of acetic acid for 2% can protect contamination of *Pennicillium* sp. and *Bacillus* sp [27].

Bacterial cellulose can either be produced under static or agitated conditions. For static conditions, a pellicle of bacterial cellulose is formed between the interface of liquid and air and thicker with cultivation time. Hestrin and Schramm reported that the pellicles were formed only at the surface of liquid that contact with oxygen. The pellicles were described as reticulated structure of nanofibers and overlapping, while others were sunk to the bottom. This mean that the yield of cellulose pellicle was produced by cell is directly proportional to the surface of culture medium but not up to the height and volume [29].

The microstructure morphology of BC product under agitated conditions is different from static condition. It has been reported as an irregular pellet well-dispersed in slurry and homogeneously dispersed in the culture medium. BC under agitated condition got a lower Young's modulus, a higher water holding capacity and

a higher suspension viscosity in the disintegrated form than BC produced in static culture [30]. The yield of cellulose under static condition was less than that under agitated condition due to the time for production was longer. When the rate of air increased in agitated conditions, it was founded that the yield of cellulose was decreased [31].

2.3 Natural rubber

The major commercial source of natural rubber latex is *Hevea brasiliensis*. Raw natural rubber from the rubber tree is thick white, circle sphere particle 0.01 – 5 micro meter (μm), density 0.975 - 0.980 gram per cubic centimeter (g/cm^3), 30 wt% of dry rubber suspended in solution. For the centrifugation process natural rubber will be concentrated to 60 wt% of dry rubber called concentrated latex. Normally the latex is added with ammonia to preserve the condition of latex life longer.

a) Isoprene b) cis-1-4-polyisoprene

Figure 2. 5 The chemical structure of a) Isoprene and b) cis-1-4-polyisoprene

The chemical structure of natural rubber is cis-1, 4-polyisoprene. There are 11,000 to 20,000 isoprene units (C_5H_8) in a polymer chain of natural rubber. NR can be excellently dissolved in non-polar solvents, for example, hexane, benzene toluene etc. The configuration pattern is amorphous structure but it can be arranged likes a crystal at low temperature. In other words, when the temperature rises, the structure is soft and sticky and when the temperature is down, the structure is tough and it becomes an elastic solid. Therefore, NR can be used in a limited temperature range. Many solvents can dissolve NR easily. Raw NR has low tensile strength and low abrasion resistance. After the vulcanization process, tensile strength will be improved to 20 MPa and elongation at break will be up to 500% - 1000% at operating temperature -40 to 70 °C.

Table 2. 2 Composition of NR [32]

Components	Concentration (%w/w)
Dry rubber contents	30-40
Protein constituents	1.90-2.5
Resin constituents	1.0-2.5
Fats and related compounds	0.9-1.0
Sugars	1.0-1.5
Water	55-65

The application of raw NR is limited, since it has low mechanical strength, non-resistance to high temperature and fast degradation under the light oxygen ozone and heat. The double bond in NR molecular is high sensitive to react with oxygen and ozone by heat and light activator. The addition of anti-degradants is widely used in NR compounds to extend the useful life. Products from NR are such as latex gloves, condom, rubber band, balloon, silicone nipple, rubber tube, latex adhesive etc.

Particle of natural rubber consist of a unit of isoprene (C_5H_8). It is connected together to present cis-1, 4-polyisoprene in the shape of sphere. Then, the rubber was covered by the phospholipid and protein. At the terminal chain end of phospholipid consist of two active functional group. The **α**-terminal group presented Mono- or diphosphate whereas the **ω**-terminal group consists a modified dimethylallyl group [33]. The negative charge of rubber particle is made up from protein membrane that surrounds the rubber molecule. It repels each other molecule and suspend in the water.

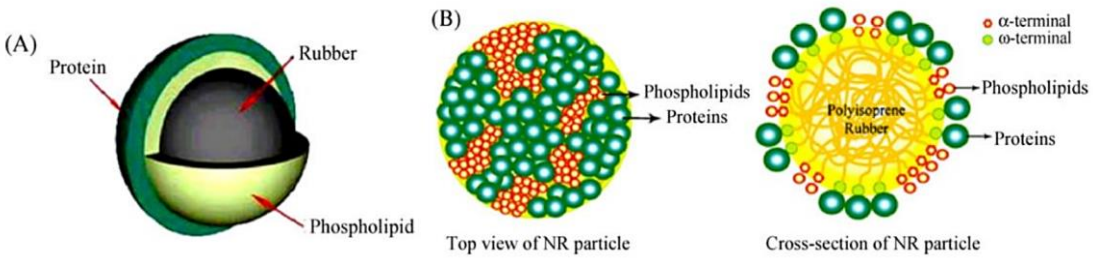

Figure 2. 6 composition of natural rubber molecule [34].

Proteins are organic compounds. Basic structure of protein is a chain of amino acid with main composition carbon, hydrogen, oxygen and nitrogen. 50% of protein exists in a serum fraction and 25% of protein surrounds at a surface particle of NR. Normally, Alpha-helix is the basic structure sheets; on the other hand, the destruction of secondary and tertiary structure changes alpha-helix into uncoil and a random shape. A variety of reagents and conditions can cause denaturation. The most common factor that denature proteins includes:

- Changes in temperature

Heat can be used to disrupt hydrogen bonds and non-polar hydrophobic interactions because of the vibration of molecules rapidly caused by kinetic energy [35].

- Changes in pH

The physiological pH of proteins is above their isoelectric points. The net negative charge from amino acid will repel each other. When the pH is adjusted to equal isoelectric points, the net charge will be zero. The force between same charge decrease whereas the gravity of different charges are equal. It can cause irreversible precipitation of protein. At the pH is lowered far below the isoelectric point, the net charge of amino acid is positive charge. The unfolding of protein occurs due to the intramolecular repulsion at the area of large charge density. The effect of high pH is analogous to those of low pH. A large negative charge are also stabilize the protein structure and even aggregation [35].

- Alcohol disrupts hydrogen bonding

The concentration of alcohol solution at 70% is used as a disinfectant on the skin because it is able to penetrate the bacterial cell wall and denature the proteins and enzymes inside of the cell. On the contrary, a 95% alcohol solution merely coagulates the protein on the outside of the cell wall and prevents any alcohol from entering the cell. Alcohol denatures proteins occurred by disrupting the side chain intramolecular hydrogen bonding. New hydrogen bonds are formed instead between the new alcohol molecule and the protein side chains [35].

- Agitation

External force by agitation is a result to stretch the polypeptide chain and break a bond [35].

Mainly protein on natural rubber particle is **α**-globulin. The Isoelectric point of amino acid which protects the natural rubber latex particle is approximately pH 4.6 [36]. The acids commonly used as coagulants are formic, acetic, oxalic and sulphuric acid

The bimodal molecular weight distribution (MWD) was confirmed by Gel-permeation chromatography (GPC) [37]. The particle diameter of NR latex contains a spread of size which it is depend on various type and age of the rubber trees; however, it is not different for fully matured of rubber trees between 0.04 – 4 μm [38]. A light Scattering Analytical Method was used to confirm the bimodal distribution of rubber particle. The rubber particles in the total cream rubber observed two peaks in the regions of 0.3 μm and 1 μm with a mean diameter of 1.07 μm. After a cream rubber was separated by centrifugation process, unimodal distribution was demonstrated that 2 groups of mean particle size. There are 1 μm of the diameter and less than 0.3 μm [39]. A spread of particle size in cream fraction was in range of 0.1 – 3 μm with the average particle diameter of 1.03 μm. On the other hand, unimodal distribution in the range of 0.05 – 3 μm was founded in serum fraction with the average diameter of 0.13 μm. [40].

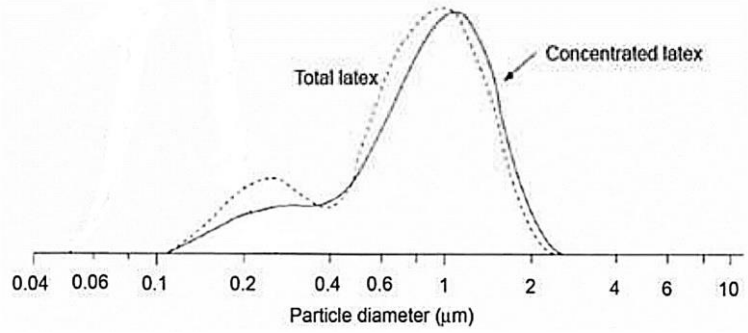

Figure 2. 7 Particle size distribution of concentrated latex [41].

2.4 Ethanol

Ethanol or ethyl alcohol is an organic compound. The functional group of alcohol is hydroxyl group (-OH). It can be produced by the fermentation of sugar by yeasts, or by petrochemical processes. The structure of ethanol is similar to water (H_2O) but hydrogen atom of water will be replaced by ethyl group (C_2H_5) so the chemical structure is C_2H_6O. The property is colorless liquid at room temperature, volatile, flammable and miscible with water. The boiling point and dipole moment of ethanol is 78.24 ℃ and 1.69D, respectively [42].

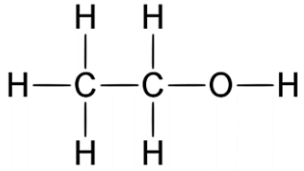

Figure 2. 8 Chemical structure of Ethanol

From the chemical structure of ethanol (Fig.2.8), it consists of hydrophilic structure (-OH) and hydrophobic structure (C_2H_5). Ethanol represented the same properties as methanol. However, ethyl group showed higher hydrophilic properties and more soluble in non-polar solvent. The differentiation number of carbon atom in alcohol can represent the different level of dissolve in water. For instance, carbon 1-3 atom alcohol can miscible in water but carbon 4 atom make the larger molecules and immiscible in water.

2.5. Modification of bacterial cellulose

Bacterial cellulose has been supplied many branch, for example, artificial skin for patient with burn an ulcers [2], bacterial cellulose for paper industry [3], drug delivery, tissue engineering [5], cardiovascular tissues [6], artificial skin for wound healing [7] etc.

BC has a high potential for use in many medical applications. Because of the highly porous structure of BC, high mechanical strength, it could be applied as a matrix for the transdermal delivery of active compounds [43-45]. There are several researches which were studied about the embedding of active compounds into the BC

2.5.1. Immersing bacterial cellulose with another solution

Maneerung, Tokura et al [46] studied on the subject of impregnation of silver nanoparticles into bacterial cellulose for antimicrobial wound dressing. The main method was studied by In-situ polymerization. Bacterial cellulose pellicles was immersed in 0.01 M of the aqueous $AgNO_3$ for 1 h, followed by rinsing with ethanol for 30 s. After that, it was reduced in $NaBH_4$ and followed by freeze-drying process. The result showed ether oxygen and hydroxyl group of bacterial cellulose fiber tightly anchor to silver ion via ion-dipole interaction and surface metal atom of stabilized silver nanoparticle.

Kingkaew, phisalaphong et al [47] studied on the subject of development of bacterial cellulose nanocomposite film for medical applications. The objective is to developed bacterial cellulose – chitosan (BCC) and bacterial Cellulose-*Aloe vera* (BCA). Immersing the purified BC pellicle into chitosan acetic acid solution and *Aloe vera* gel for 36 h rinsed in distilled water air-dried at room temperature. The result in case of BCC film has the intermolecular interaction between BC and chitosan, which the mechanical properties, the crystallinity, the water absorption capacity, the water vapor transmission rate, the oxygen transmission rate and the average pore diameter were decreased when prepare to BC. While the mechanical properties, the crystallinity, the average pore diameter of BCA film were decreased, the oxygen transmission rate and the antifungal ability against *Aspergillus niger* were enhanced. BC film by immersing into chitosan solution and *Aole vara* gel exhibited advantageous properties to use as wound dressing material.

Cai and Kim [48] studied on the subject of Bacterial cellulose/poly (ethylene glycol) composite: characterization and first evaluation of biocompatibility. Immersing bacterial cellulosed pellicle into the poly ethylene glycol (PEG) aqueous solution. After that, drying by freeze-drying process. The result showed that BC/PEG has very well interconnected porous network structure and large aspect surface. The thermal stability was improved but the Young's modulus and tensile strength tended to decrease.

Gea, Bilotti et al [20] studied on the subject of Bacterial cellulose–poly (vinyl alcohol) nanocomposites prepared by an in-situ process. Impreg-BC was produced by impregnation of bacterial cellulose pellicle with 100 ml of the PVA solution overnight and pressed (115 ℃ for 5 min at 70 MPa) into a sheet. In-situ BC was prepared by PVA solution added directly into the medium of the growing BC. Then, In-situ BC was rinsed fresh water and dried at room temperature. Investigate the morphology and mechanical properties of impregnate-BC and in-situ BC. The results show that the behavior of PVA in BC acts as a plasticizer which interrupting hydrogen bonding between cellulose fibrils within the BC network. In addition, in-situ BC was effected more than the impregnate BC due to a minor change in the dimension of BC ribbons. As a result, the Young's modulus of insitu-BC was reduced while the toughness was increased when compared to pure BC sheet.

Leitão, Silva et al [49] studied on the subject of production and characterization of a new bacterial cellulose/poly (vinyl alcohol) nanocomposite. Investigated the effect of the addition of PVA and oven drying on the morphology and mechanical property of BC/PVA membrane. The method was immersing purified bacterial cellulose into 10% PVA solution (Mw = 900 Da, 8,000 Da, 35,000 Da, 100,000 Da) for 24 h at 80 ℃ and frozen the membrane at -20 ℃ for 24 h. After that, poured the membrane in distilled water and wash to removed excess PVA. Dry BC and BC/PVA sample were dried in oven at 50 ℃ 12 h. SEM photograph showed the portion of the membrane contained large pores and the diameter was in range of 500 nm to 2 μm. The distribution of PVA into BC membrane was non-uniform induce the Young's modulus and tensile strength of dry-BC decreases.

Jewprasat and phisalaphong [50] studied on the subject of pervaporation of ethanol water mixtures using bacterial cellulose-poly (vinyl alcohol) membrane. The method was immersed BC hydrogel into PVA solution at 5, 7, 10 and 12% (w/v) at 60 ℃ in 7 days. The results showed that the membrane was highly hydrophilic than BC membrane. The film 10 % PVA showed very good mixing of both component; moreover, the result showed highest crystallinity when compared with other

concentration of BC-PVA/GA membrane and more elastic behavior than BC membranes. The report after cross-linked with glutaraldehyde showed lower crystallinity, tensile strength and Young's modulus compared to these without the cross linking but higher than those of BC membranes.

Taokaew, Nunkaew et al [51] studied on the subject of containing ethanolic extract of mangosteen peel. BC films was immersed into 100 ml of the ethanolic mangosteen extracts solutions at 0.01, 0.1, 1% v/v under ambient conditions for 24 h. After that, rinsing with 20% v/v ethanol solution. Then, the composite films were dried at room temperature and investigated for the morphology by SEM. The results showed that the extract particles were observed between the film layers. The extract particle not only filled in the pores of BC but penetrated into the network also. the extract particles showed hydrophobic properties. Water absorption capacity (WAC) of the modified film was lower than unmodified BC film due to the hydrophobic properties of the mangosteen extract.

Suratago, Taokaew et al [52] studied on the subject of development of bacterial cellulose/alginate nanocomposite membrane for separation of ethanol-water mixtures. BC hydrogel was modified by immersing in sodium alginate solutions of concentration 1, 2, or 3% (w/v) at 50 ℃ for 5 days. After that, the films were rinsed with DI water and cross-linked with 5% (v/v) calcium chloride for 3 h. Then the films were rinsed again and dry at ambient air. The results showed that the increasing of thickness of BC membrane depend on the concentration of alginate incorporation into the BC layer. The thickness of the unmodified BC was 50 μm then increased to 130, 180 and 322 μm respectively. On the contrary, the surface area and pore diameters of the membrane decreased with increasing alginate content. The tensile strength and Young's modulus were decreased; whereas, the elongation at break was increased.

2.5.2 Bacterial cellulose and Natural rubber composites

Rungjang, sukyai et al [53] studied on the subject of bacterial cellulose filled natural rubber composites. The objective was develop a new material from bacterial

cellulose and natural rubber then investigate the influence of bacterial cellulose powder and bacterial cellulose nanowhiskers (BCNWs) on the thermal, mechanical and chemical properties of natural rubber composites. The method was separated 2 case of mixing. In the first case, mixed BC powder and NR latex by a laboratory two roll mill. In the second case, the suspension of BCNWs and NR latex were mixed with 0-15% weight fraction of solid BCNWs in NR latex and stirred for 8 h, then films were dried at 40 ℃ 8 h. Investigated the modulus, hardness of BC/NR latex composite. The hardness increased when increasing BC filler loading but it depends on appreciable change in cure time. The effect of BCNWs loading on tensile strength and modulus showed that the highest stiffness of BCNWs/NR nanocomposites improvement at 7.5% BCNWs loading. Elongation at break of BCNWs/NR nanocomposites were decreased with increasing BCNWs filter loading.

Trovatti, Capote et al [54] studied on the subject of development and characterization of natural rubber and bacterial cellulose-sponge composites. The method was added 0.2 g of bacterial cellulose nanofiber (suspension at 0.5 wt %) then mixed with 8 g of NaCl and 1 g of natural rubber latex (45 wt % solid content). The mixture was dried in oven at 30 ℃ then removed the salt by deionized water and freeze dried to removed water. The results showed the homogenously reinforcement of BC fiber into the natural rubber matrix. The physical properties of composite films were changed by the reinforcement of BC fiber due to changing of the porous structure of material. In conclusion, the composite films showed good water affinity which increased mechanical properties.

2.5.3 Effect of ethanol on gel fraction of NR latex particles

Tarachiwin et al [55] studied on the subject of structural characterization of **α**-Terminal group of natural rubber. Decomposition of branch-points by phospholipase and chemical treatments. The method is the deproteinized rubber latex(DPNR) was add 1% v/v ethanol and stirred at room temperature compared to the DPNR treatment with another chemical. The result show that the addition of 1% v/v ethanol in DPNR dispersion led to decrease molecular weight and narrower MWD. It can be deduced

that the addition of ethanol in DPNR solution resulted in the decomposition of branch–points caused by hydrogen bonding between phospholipids and proteins.

Sakdapipanich et al [41] studied on the subject of molecular structure of natural rubber and its characteristics based on recent evidence. It was reported that NR contains both soft-gel and hard-gel [56]. The soft-gel fraction on NR decreases by deprotinization with proteolytic enzyme. It can be partly decomposed in solution by adding small amouts of a polar solvent in a good solvent and almost completely solubilized by transesterification. The gel fraction decreased when adding 2% v/v ethanol in the rubber solution. The gel fraction completely decomposed after transesterification precess.

2.5.4 Effect of ethanol on protein

The effect of organic solvents on the structural properties of protein may be several affected. However, there are various researcher study the effect of organic solvent and report as follow;

Van Koningsveld, G.A., et al. [57] studied on the subject of effect of ethanol on structure and solubility of potato proteins and the effects of its presence during the preparation of a protein isolate. It was reported that unfolding of proteins because ethanol treatment can also influence the solubility characteristics and the functional properties of proteins. The presence of ethanol considerably decreases the denaturation temperature of potato proteins.

Roberts, R. and D. Briggs [58] studied on the subject of characteristics of the various soybean globulin components with respect to denaturation by ethanol. The sample of the wet-precipitated soybean globulins, at pH 5.0, were mixed with 40 ml. aqueous ethanol solution in the range of 10-100% ethanol and left in contact for a period of 8 h. The total amount of protein denaturation was measured as the proportion of buffer insoluble protein formed. It was observed that maximum denaturation occurred nearly at 60% ethanol and decreased rapidly with increasing ethanol concentration.

Wolf et al. [59] studied on the subject of physical properties of alcohol-extracted soybean proteins. They referred to previous research from Smith et al. reported the alcohol concentration, cause of the most extensive protein denaturation, were 50-70% for methanol, 30-60% for ethanol and 30-50% for isopropanol. The experiment results show that the soybean proteins were sensitive to treatment with aqueous alcohols. Maximum loss of protein solubility in soybean meal occurs at alcohol concentrations of 40-60%. The decrease in solubility of the entire acid-precipitated proteins upon 2 h.; therefore, decreasing of insolubility might be effected by minimizing extraction time with high concentrations of alcohol.

CHAPTER 3
EXPERIMENTAL

3.1 Materials

3.1.1 Microbial strains

The *A. xylinum* (AGR60) was isolated from *nata de coco*. The stock culture was kindly supplied by PramoteTammarat, the Institute of Food Research and Product Development, Kasetsart University, Bangkok, Thailand.

3.1.2 Chemicals substances

The details of chemicals used in this experiment are shown in Table 3.1

Table 3. 1 The chemicals used in this experiment

Chemical	Supplier
Sucrose	Ajax Finechem
Ammonium sulfate	Ajax Finechem
Sodium hydroxides	lobachemie
Acetic acid	QRëC
Ethanol absolute	QRëC

3.1.3 Natural rubber latex 60% drc

The composition of natural rubber latex (NRL) 60% drc, which was purchased from the Rubber Research Institue of Thailand, Kasetsart University were shown in table 3.2.

Table 3. 2 composition of NRL 60% drc

Components	Concentration (wt.%)
Dry rubber contents	20-25
Protein constituents	1.5
Resin constituents	2.0
Carbohydrate constituents	1.0
Inorganic substances	0.5
Water	55-65

3.1.4. Equipment

- Scanning electron microscopy, SEM (JEOL JSM-7610F, Japan).
- Fourier Transform Infrared (FTIR) spectrometer (Nicolet SX-170, USA).
- Universal testing machine (ASD8-82A.TSX, UK).
- X-ray Diffractometer (D8, Karlsruhe Germany)
- Differential scanning calorimeter (NETZSCH DSC 204 F1 Phoenix)
- Mastersizer3000 (Malvern, United Kingdom)
- Autoclave (Model Tomy Autoclave SS-325, Nerima-ku, Tokyo, Japan).
- Oven (SNOL 58/350, Lithuania)
- Balance (Mettler-Toledo GmbH lm Langacher 44 8606 Greifensee Switzerland)
- Biosafety carbinets (Laminar flow cabinets)

3.2 Film preparation

The medium for the inoculum was coconut-water supplemented with 5.0% sucrose, 0.5% ammonium sulfate and 1.0% acetic acid. The medium was sterilized at 110 ℃ for 5 mins. Precultures were prepared by a transfer of 50 ml stock culture to 1000 ml in 1500 ml bottle and incubated statically at 30 ℃ for 7 days. After the surface pellicle was removed, a 5% (v/v) preculture broth was added to sterile medium and statically incubated at 30℃ for 5 days in a Preti-dish. All sample BC pellicles were purified by washing with DI water 30 minutes and then was treated with 1% NaOH (w/v) at room temperature to remove bacterial cells for 24 hours, followed by a rinse with water for 2 hours to remove excess bacterial cells and pH became to 7. The BC membranes were kept in DI water until used.

The BC membranes were immersed in 300 ml natural rubber dispersion at 0.5, 1.5, 2.5, 5, 7.5 and 10% (Table A.1). Then, 6 ml of 50% (v/v) ethanol was added into NR dispersion which was the optimum ratio from preliminary study (Appendix A (2)). Each solution was poured in the tray. After that, the immersion temperature was investigated at 30, 50, 60 and 70^{o}C. BC membranes in the tray was immersed with NR dispersion until it was saturated (48 hours). Then composite films were washed with distillate water, air-dried at 30℃ and stored in plastic film at room temperature.

3.3 Characterization of NR-BC films

3.3.1 Field emission scanning electron microscopy (FESEM)

The examination of the surface morphology was performed by Field emission scanning electron microscopy (FESEM). Scanning electron micrographs were taken with JEOL JSM-7610F (Tokyo, Japan) microscope at Scientific and technological research equipment centre (STREC), Chulalongkorn University. The composite films were frozen in liquid nitrogen, immediately snapped, and vacuum-dried. Then, the membranes were sputtered with gold and photographed. The coated specimens were kept in dry

place before experiment. The FE-SEM was obtained at 10 kV which was considered to be a suitable condition since too high energy can be burnt the samples.

3.3.2 Laser particle size distribution (PSD)

The particle size of natural rubber latex (NR) and natural rubber latex with ethanol were investigate by laser diffraction technique. Particle size distribution curve were taken with Mastersizer3000 (Malvern, United Kingdom) at Scientific and technological research equipment centre (STREC), Chulalongkorn University. The operating size classes were recorded in the range of 0.01 – 3000 μm with stirrer speed achieved 2000 rpm.

3.3.3 Fourier Transform Infrared Spectroscopy (FTIR)

The chemical structure of the composite films were analyzed and recorded by FTIR with a Nicolet FT-IR Spectrometer SX-170 (Thermo fisher scientific, USA) in the region of 4000–500 cm^{-1}, at Scientific and technological research equipment centre, Chulalongkorn University.

3.3.4 Water absorption capacity (WAC)

Water absorption capacity was determined by immersing the pre-weight of dry BC film in DI water at room temperature until equilibrium. Then the film was removed from the water and blotted out with Kim wipes. The weight of the reswollen film was measured, and the procedure was repeated until there was no further weight change. Water content was calculated by using the formula

$$WAC\% = \left[\frac{W_h - W_d}{W_d} \right] \times 100$$

Where W_h and W_d denoted the weight of hydrate and dry films, respectively

3.3.5 Toluene uptake (TU)

The BC and NR-BC composite films were prepared with dimension 20 x 20 mm^3. Then, the specimen was weighed and immersed in toluene at room temperature until the specimen saturated. After that, the composite films were weighed and repeated the procedure until there was no further weight change. The toluene uptake was calculated by using this formula

$$TU\% = \left[\frac{W_t - W_0}{W_0} \right] \times 100$$

Where W_0 and W_t denoted the weight of dry films before swelling and after the time (t) of immersion, respectively.

3.3.6 X-ray diffraction (XRD)

The examination of the structure of crystalline materials was performed by X-ray Diffractometer (D8, Karlsruhe, Germany) at Department of Materials Science, Faculty of Science, and Chulalongkorn University. The determination of crystalline property was done under BC membrane was cut into strip-shaped specimens 4 cm in width and 5 cm in length. The operating condition were performed in the 2θ range of 5-40 using Cu Ka radiation.

3.3.7 Differential Scanning Calorimetry (DSC)

DSC was used to identify the performance of the composite films for instance, glass transition temperature (T_g), crystalline melt temperature (T_m). Sample about 3-5 mg was sealed in aluminum pan. Then sample was subject to DSC measurement under nitrogen gas. In addition, evaluate the curing behavior of composite films was determined by using NETZSCH DSC 204 F1 Phoenix (NETZSCH, Germany). The thermal scanning was heated up from -100 to 400 °C and with a heating rate of 5 °C/min

3.3.8 Thermal gravimetric analysis (TGA)

The thermal weight change of BC, NR and composite films were performed by using thermal gravimetric analyzer (Q50 V6.7 Build 203. Universal V4.5A TA). The thermal scanning was heat from room temperature of 30 °C to 700 °C. The heat rate was 10 °C/min. The weight of each samples were used around 10 mg under nitrogen gas. The percent weight loss was plotted against temperature.

3.3.9 Mechanical properties testing

In this study, the tensile strength of the membrane was measured by Instron Testing Machine (ASD8-82A.TSX, NY, USA) at Scientific and technological research equipment centre, Chulalongkorn University. The test conditions follow ASTM D882. The determination of tensile property was done under BC membrane was cut into strip-shaped specimens 10 mm in width and 10 cm in length. At least five specimens were used for each blend composition.

3.3.10 Biodegradation in soil

Biodegradation of BC and NR-BC composite films was buried in the pot of soil for 2 months. The samples were cut in the form of 3 x 3 cm^2 and buried under the soil of 10 cm uncontrolled conditions. Temperature and humidity change as the weather during the day. After 1 and 2 months, the samples were taken out, washed with distilled water, and dried at 50°C 24 h and then weighed. The specific biodegradation rates based on the mass loss of films and calculated by using this formula

$$\text{Biodegradation (\%)} = \left[\frac{W_1 - W_2}{W_1} \right] \times 100$$

Where W_1 and W_2 denoted the initial dry weight of the samples (g) and the residue dry weight of films after biodegradable in soil, respectively.

CHAPTER 4

RESULTS AND DICCUSSION

Bacterial cellulose (BC) was produced by *Acetobactor xylinum* in the coconut-water based medium under static culture. The diameter of BC film was about 14 cm as shown in Figure 4.1. NR-BC composite films were prepared by immersing BC membrane into NR dispersion in the range of 0-10% at various temperatures of 30°C, 50°C, 60°C and 70°C. The effects of NR concentration and immersion temperature were investigated. The definition of BC referred to the unmodified BC. While XXNR-BCYY composite films, XX and YY refer to the concentration of NR dispersion (0.5, 1.5, 2.5, 5, 7.5, and 10%) and the immersion temperature, respectively. To demonstrate, 0.5NR-BC50 referred to the immersion of BC into 0.5% NR at 50°C.

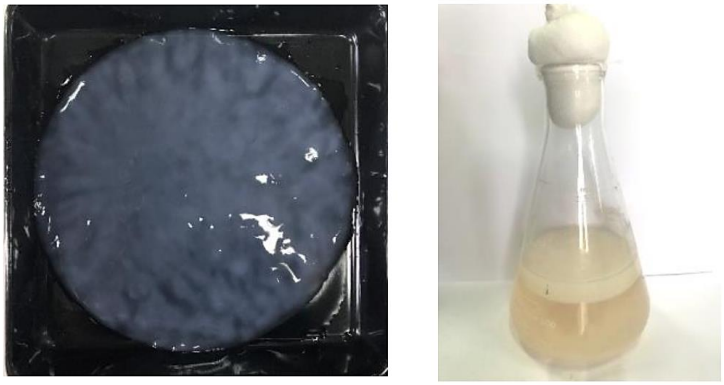

Figure 4. 1 Bacterial cellulose incubation under static condition and stock culture

For the first part, the morphology, the particle size distribution of natural rubber latex,chemical composition, physical properties and the crystallinity of composite films were examined to confirm the occurrence composite material by Field Emission Scanning Electron Microscopy (FESEM), Particle Size Distribution (PSD), Fourier Transform Infrared Spectroscopy (FTIR), Water Absorption Capacity (WAC), Toluene Uptake (TU) and X-ray Diffraction (XRD) respectively; Then, compared with those of unmodified BC and NR-BC composite films. In the second part, to investigate the end-use properties of composite material as mechanical properties (tensile strength, Young's modulus and elongation at break) and thermal properties (T_m, T_g) then the

biodegradable of the composite films in soil were investigate by the mechanical properties testing, Differential Scanning Calorimetry (DSC) and Biodegradable in soil.

4.1.1 Field Emission Scanning Electron Microscopy (FESEM)

The morphology and cross section of pure BC and the composite films were characterized by Field Emission Scanning Electron Microscopy (FESEM) as shown in Figure 4.2-4.7. The thickness of dry BC films and NR-BC composite films were measured by ImageJ program and shows in Table 4.1

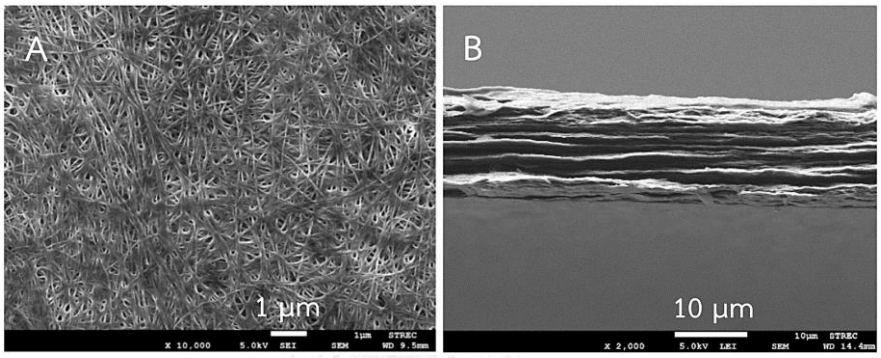

Figure 4. 2 FESEM images of the dried BC film; surface at magnification of 10,000x and scale bar represent 1 µm (A) cross-section at magnification of 2000x and scale bars represent 10 µm (B)

From Figure 4.2, the surface of dry BC film consist of the dense structure of nanocellulose fiber, the average diameter of nanocellulose fibers was approximated 50-100 nm [43] that cross-linked in three-dimension space. The porous between cellulose fibers dispersed in the structure of a thin film. The cross-section of dried BC film demonstrating that the dense layer of dry nanocellulose structure by losing water in the structure; this cause affect to fiber shrink and more compact. The average thickness of the unmodified dry BC was approximated by 0.012 mm. (12 µm).

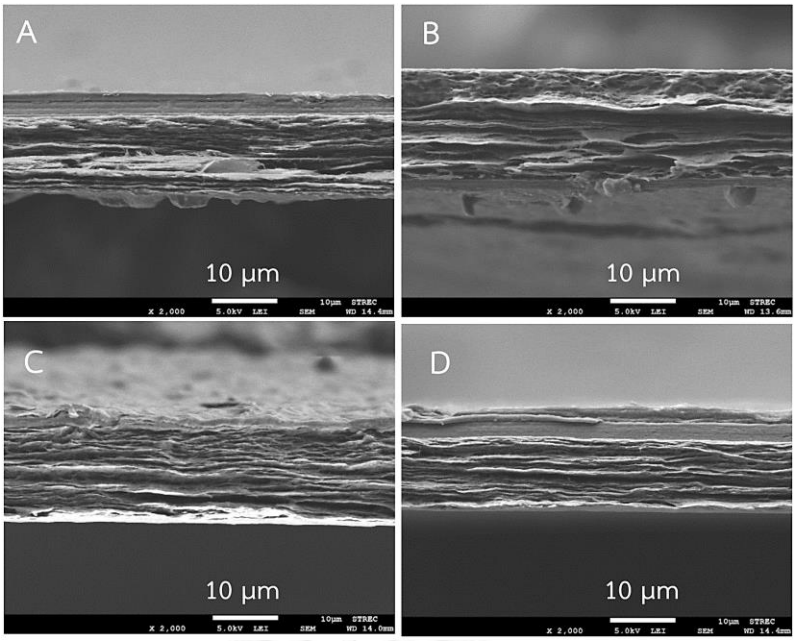

Figure 4. 3 FESEM images of the cross section of 0.5NR-BC30 (A), 2.5NR-BC30 (B), 5NR-BC30 (C) and 10NR-BC30 (D) at magnification of 2000x. The scale bars represent 10 µm.

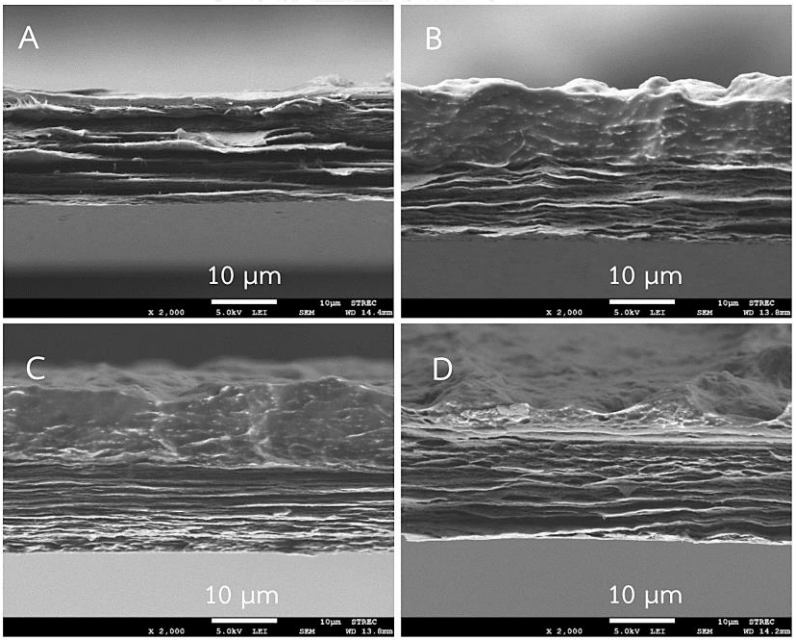

Figure 4. 4 FESEM images of the cross section of 0.5NR-BC50 (A), 2.5NR-BC50 (B), 5NR-BC50 (C) and 10NR-BC50 (D) at magnification of 2000x. The scale bars represent 10 µm.

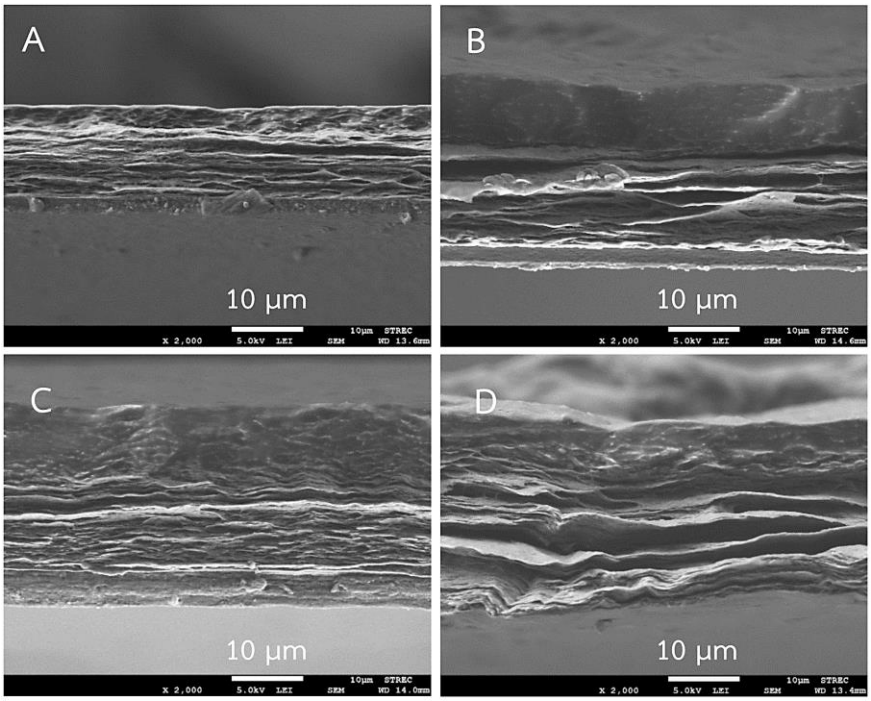

Figure 4. 5 FESEM images of the cross section of 0.5NR-BC60 (A), 2.5NR-BC60 (B), 5NR-BC60 (C) and 10NR-BC60 (D) at magnification of 2000x. The scale bars represent 10 μm.

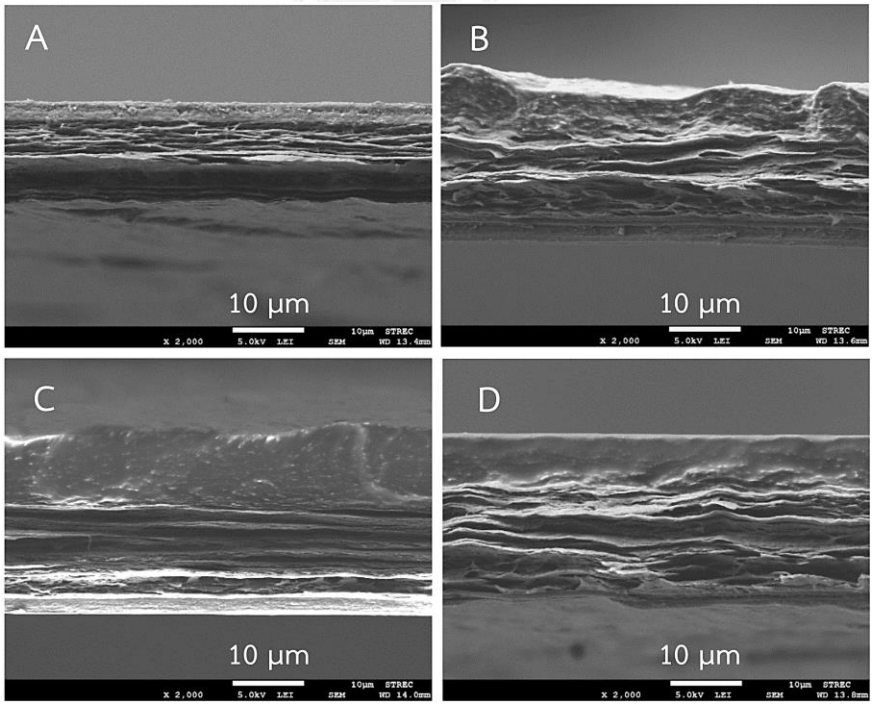

Figure 4. 6 FESEM images of the cross section of 0.5NR-BC70 (A), 2.5NR-BC70 (B), 5NR-BC70 (C) and 10NR-BC70 (D) at magnification of 2000x. The scale bars represent 10 μm.

Table 4. 1 The thickness of BC and NR-BC composites films

Samples	Thickness (μm)		Samples	Thickness (μm)	
	Average[(a)]	SD		Average[(a)]	SD
BC	12.047	0.259			
0.5NR-BC30	12.737	0.581	0.5NR-BC60	13.856	0.125
2.5NR-BC30	19.077	0.376	2.5NR-BC60	24.97	0.9
5NR-BC30	15.851	0.532	5NR-BC60	27.208	0.392
10NR-BC30	14.657	0.491	10NR-BC60	24.149	1.62
0.5NR-BC50	14.844	0.637	0.5NR-BC70	13.315	0.584
2.5NR-BC50	20.606	0.238	2.5NR-BC70	20.979	0.692
5NR-BC50	21.987	0.962	5NR-BC70	25.268	0.287
10NR-BC50	18.536	0.63	10NR-BC70	21.725	0.349

(SD: Standard deviation)

[(a)] Value are average of 3 specimens

FESEM images of the dried composite films with various NR concentration and immersion temperature were shown in Figure 4.3 - 4.6. The morphology of the dry composite films had rough surface, soft yellow-shade. The cross-section of dried composite films showed higher thickness when compared to pure BC and consisted two immiscible layers of a dense layer nanocellulose covering with a huge layer of NR. The thickness of dry BC films and composite films were measured by ImageJ program as shown in Table 4.1. The thickness of composite film was related with the amount of the NR molecules inserted into the surface of composite films. The high thickness of composite film achieved when the concentration of NR is 2.5-5%. With the increment of NR concentration up to 5% could increase the accumulation of NR molecules in the surface of BC film increased. However, the addition of NR concentration higher than 5% could affect the agglomeration of nonpolar NR molecules, since the molecules would close up to each other and had more attraction between each molecule.

Considered the effect of immersion temperature, the thickness of composite films had no significant change after the increase in the immersion temperature from

30 °C up to 70 °C at low NR concentration (lower than 2.5%). Due to the low concentration, the number of NR molecules in BC was limited, resulting in low adhesion. For the NR concentration higher than 2.5%, the thickness of composite films showed significantly increased after increasing the immersion temperature, which should be the effect from the increase the kinetic energy of NR molecules after the temperature was raised. The probability of higher agitation and collisions might be occurred on the surface of BC film. However, an amount of NR inserted into BC under the rise of the immersion temperature to 70°C was slightly reduced. At high temperature, the rubber molecules could agglomerate by higher collision into large particles, which hardly penetrated through the surface of BC film. The surface of never-dried composite films is shown in Figure 4.7.

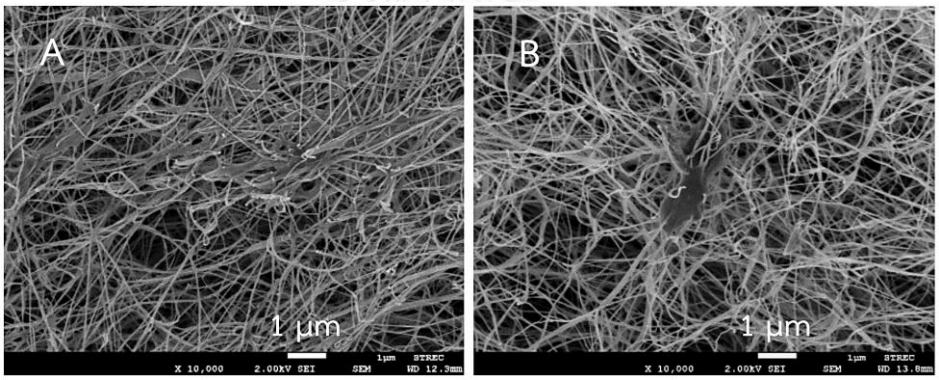

Figure 4. 7 FESEM images of the never-dried NR-BC films; cross-section of 5NR-BC60 at magnification of 10,000x (A) and 10NR-BC60 at magnification of 10,000x (B). The scale bars represent 1 µm.

As shown in Figure 4.7, the FESEM images of the composite films with 5 % and 10% NR concentration and with immersion temperature at 60 °C exhibited a few NR molecules penetrated through the pores of BC surface. The penetration of NR into BC structure was observed between nanocellulose fibers. Each fiber was linked together by NRL. The accumulation of large NR particles on the BC surface could block the transfer of smaller particles through the pore of BC. The immersion temperature would have a higher effect on the agglomeration of NR particles at BC surface rather than the activation of NR molecule penetration. However, the addition of ethanol in to the NRL solution would help dissolve some gel fraction and protein in NRL. The addition of

ethanol would also help reduce the viscosity of the NRL solution, resulting in increased penetration of NRL into BC films. The effect of ethanol concentrations on NRL molecule was further investigated by PSD.

4.1.2 Laser particle size distribution (PSD)

The characteristics of particle size distribution of NR with various ethanol concentrations as shown in Figure 4.2

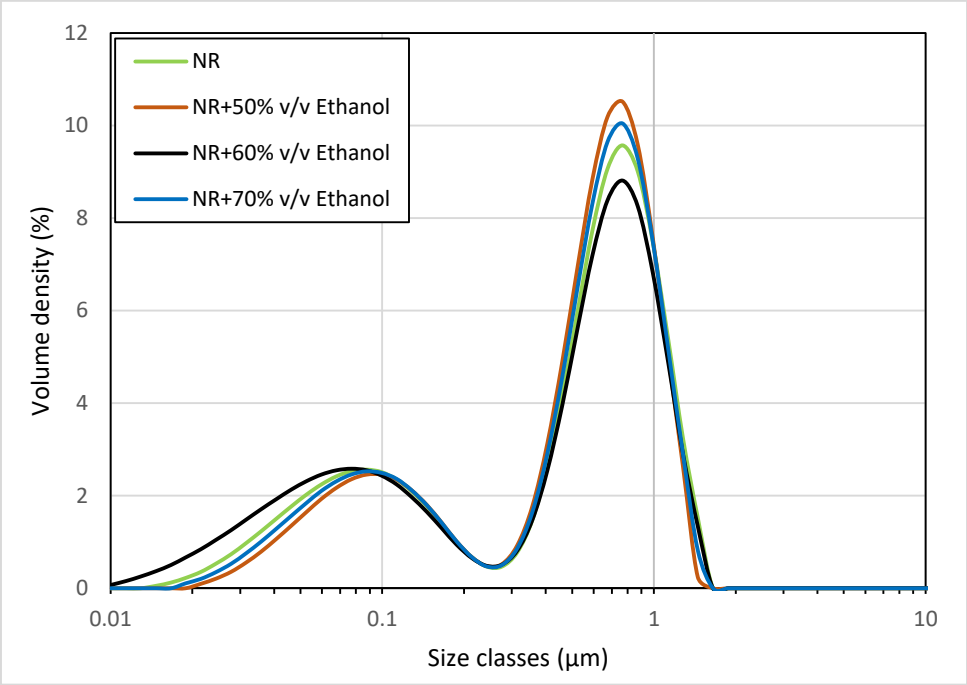

Figure 4. 8 Particle size distribution of NR with various ethanol concentrations

As shown in figure 4.8, the particle size distribution of natural rubber latex (NRL) and natural rubber latex treated with 50%, 60% and 70% v/v ethanol were in the range of 0.01 - 2 µm. The particle size distribution curve of NR shows a bimodal distribution, which had two highest points at 0.08 µm and 0.7 µm. The percent volume densities of each peak were at 2.56% and 9.57%, respectively. In comparison between particle size of unmodified NR and modified NR, the shift of low particle size distribution peak was observed after the addition of 60% v/v ethanol concentration. It was shifted to the left from a normal curve of NR, indicating the decrease in the particle size of NR. High volume density of the particle size was observed at 0.6-0.8 µm. Therefore, the addition of the small amount of polar solvent in the rubber latex solution might cause

the decomposition of the hydrogen bonding between phospholipids, proteins, or both of them at the terminal ends of the rubber chain and this effect is associated with decreasing of rubber molecule. According to some literatures, ethanol could be used to dissolve protein membrane at the surface of rubber particles [33, 55, 60]. Nonetheless, the low initial curve of particle size distribution was slightly shifted to the right when adding 50 and 70% v/v ethanol. However, the overall particle size distributions were similar to those of the unmodified NR. The occurring curve showed that ethanol slightly affects the distribution of NR particle size. At low or excessive amount of ethanol concentration could disturb the negative charge of protein membrane around the rubber particle surface. For the precipitation of rubber latex, methanol was generally used in laboratory and rubber farm [60, 61]. Likewise, ethanol can cause the coagulation of rubber because it is also an organic polar solvent (of low molecular weight alcohols). Therefore, the coagulation of NR particles into larger particles could occur under the excessive volume and concentration of ethanol. However, within the application range of this study, the addition of ethanol into NRL solution had only slightly effect on the change of size of rubber particles.

4.1.3 Fourier Transform Infrared Spectroscopy (FTIR)

The specific functional groups and chemical interaction of a pure BC and the composite films, BC with various NR concentration and immersion temperature, between bacterial cellulose and natural rubber were identified by FTIR spectroscopy exhibited in Figure 4.9 - 4.12

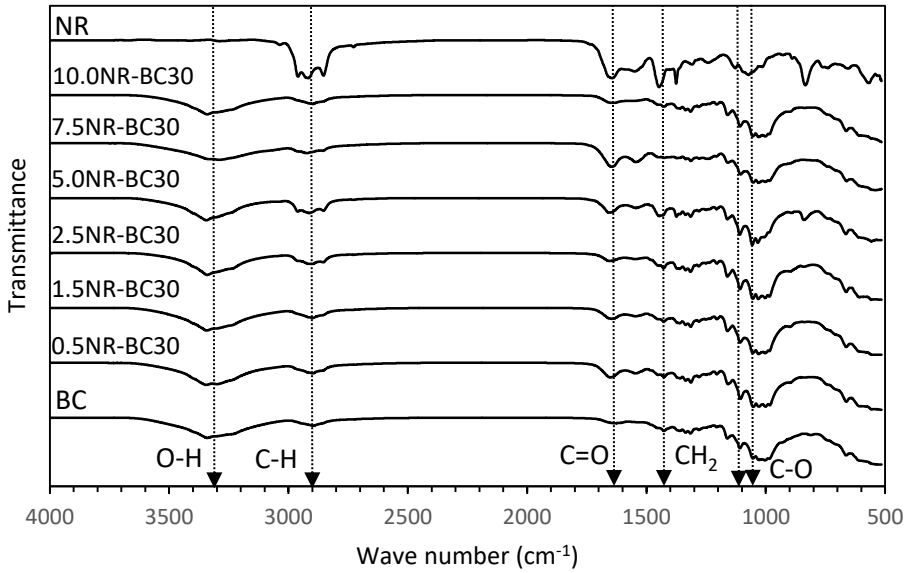

Figure 4. 9 FTIR spectra of BC and composite films at immersion temperature 30°C

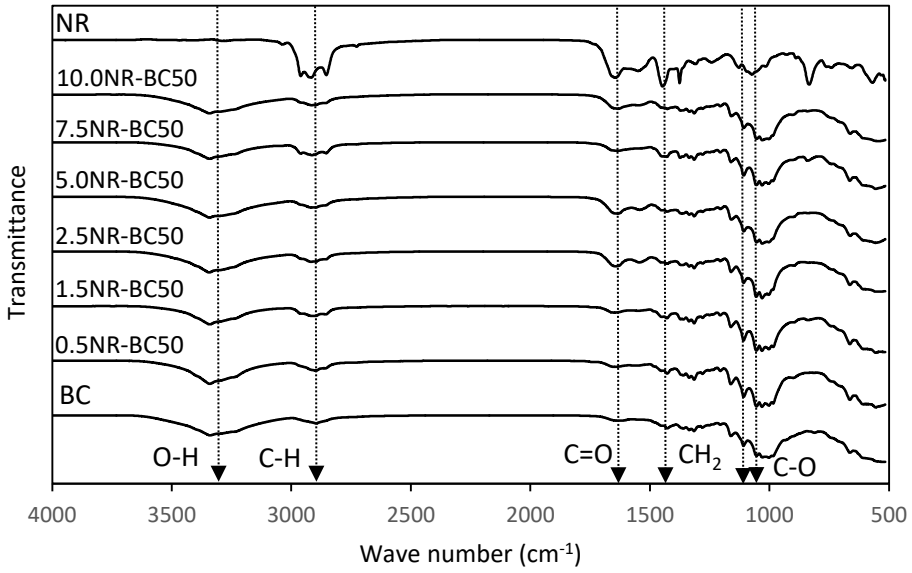

Figure 4. 10 FTIR spectra of BC and composite films at immersion temperature 50°C

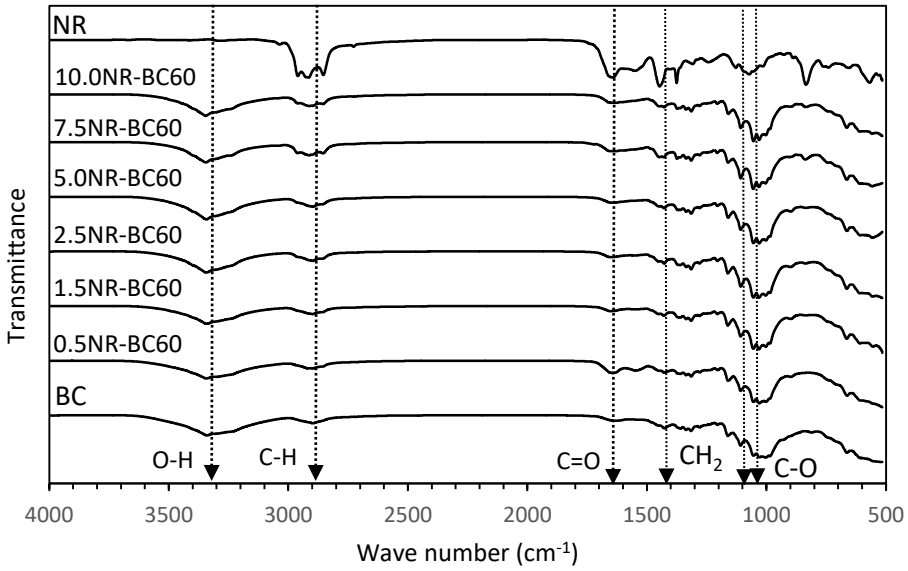

Figure 4. 11 FTIR spectra of BC and composite films at immersion temperature 60 ℃

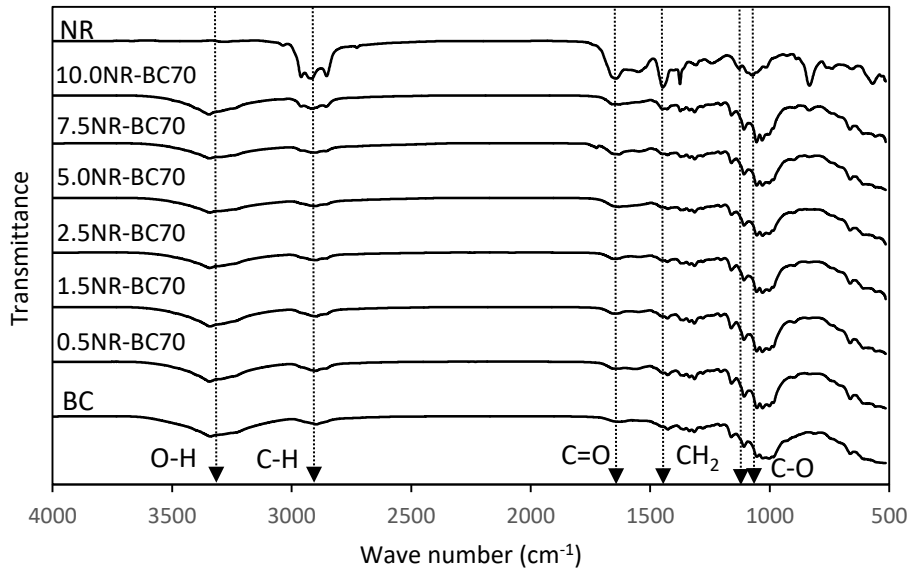

Figure 4. 12 FTIR spectra of BC and composite films at immersion temperature 70 ℃

From Figure 4.9 to 4.12, FTIR spectra of pure BC showed characteristic peak at 3347 cm^{-1} , which demonstrates the O-H stretching vibrations of hydroxyl group; 2900 to 2800 cm^{-1} indicates the vibration of C-H stretching; 1650 to 1640 cm^{-1} is attributed to the vibration of carbonyl group (-CO) in BC. The peak at 1440 cm^{-1} indicates CH_2 bending; 1165 cm^{-1} to 1060 cm^{-1} is assigned to C-O stretching In the case of pure NR, the characteristics peak of NR is shown at 2960 cm^{-1} indicating the vibration of C-H

stretching; at 2917 cm^{-1} indicating the symmetric stretching of CH_2, 2847 cm^{-1} demonstrating the asymmetric stretching of the CH_3 group; 1465 cm^{-1} indicating the vibration of symmetric bending of CH_2 ; 1375 to 1450 cm^{-1} indicating the vibration of asymmetric bending of CH_2 and the peak at 1637 cm^{-1} demonstrating the vibration of C=C stretching [62, 64]. The FTIR spectra of composite films showed the combination peaks of dependent materials from BC and NR. The slightly shift of hydroxyl peaks with the addition of NR in composite films indicates some weak physical interactions between BC and NR. No occurrence of new peak indicates no chemical interaction between those two components.

4.1.4 Water absorption capacity (WAC)

Swelling behavior can indicate the capability of liquid absorption of BC and composite films. There are several factors influence film swelling, such as network density, hydratability of films, polarity, pH etc [65]. In this research, the dried sample of BC, NR- BC composite films and NR were immersed in distilled water at room temperature until no weight gained or equilibrium swelling was reached. Water absorption capacities of BC and composite films are shown in Table 4. 2. and Figure 4.13-4.16.

Table 4. 2 The water adsorption capacity of all samples with immersion time 4 h.

Immersion temperature	Water absorption capacity (%)							
	BC(0)	0.5	1.5	2.5	5	7.5	10	NR(100)
30	610.5	206.3	131.2	170.0	187.2	258.3	288.1	10.9
50	610.5	213.9	208.2	88.4	88.6	115.9	142.5	10.9
60	610.5	314.7	289.3	143.2	124.3	174.8	173.8	10.9
70	610.5	267.4	203.5	203.8	131.0	183.5	192.6	10.9

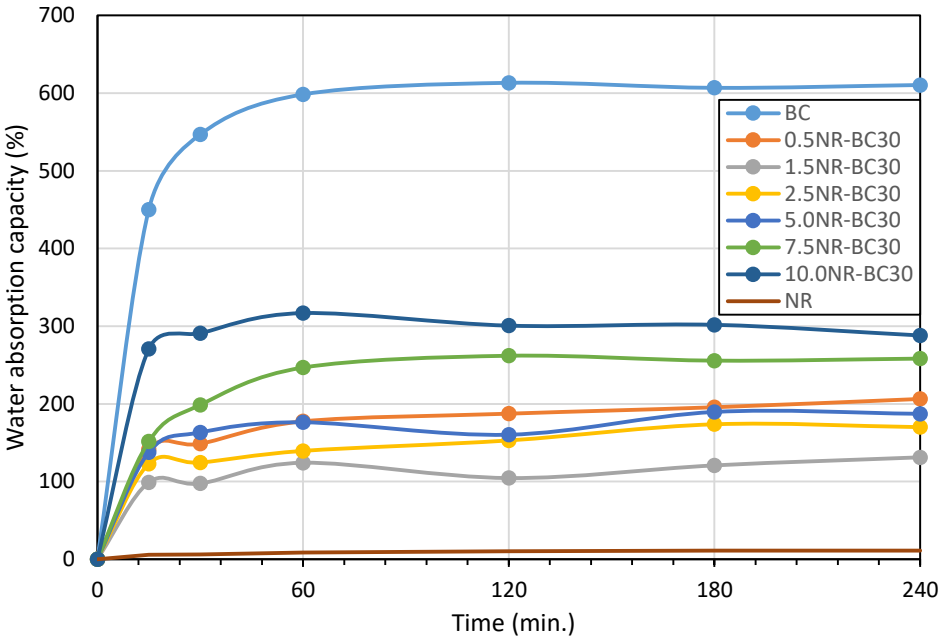

Figure 4. 13 Water absorption capacity of BC and composite films for the immersion temperature at 30 °C.

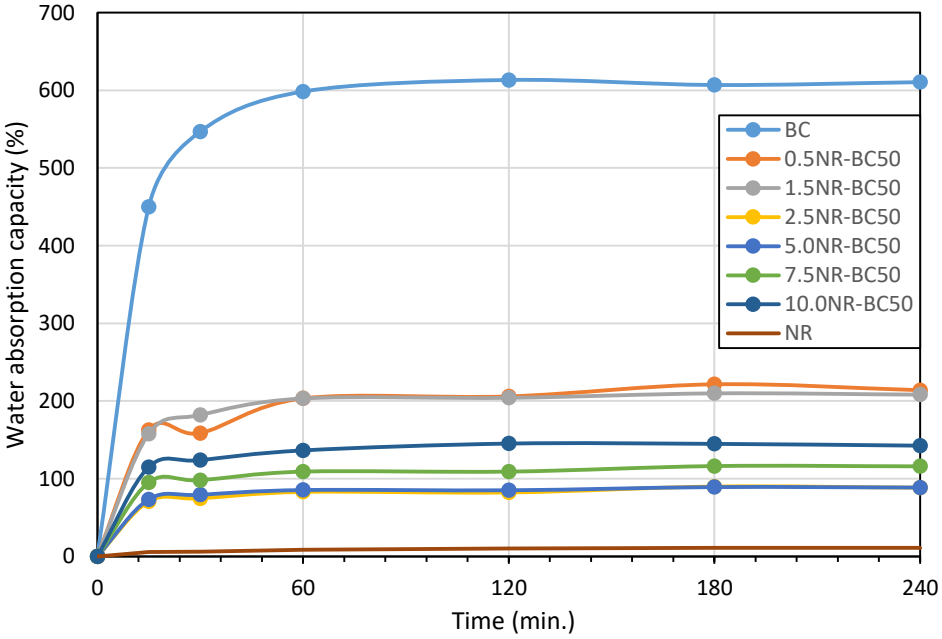

Figure 4. 14 Water absorption capacity of BC and composite films for the immersion temperature at 50 °C.

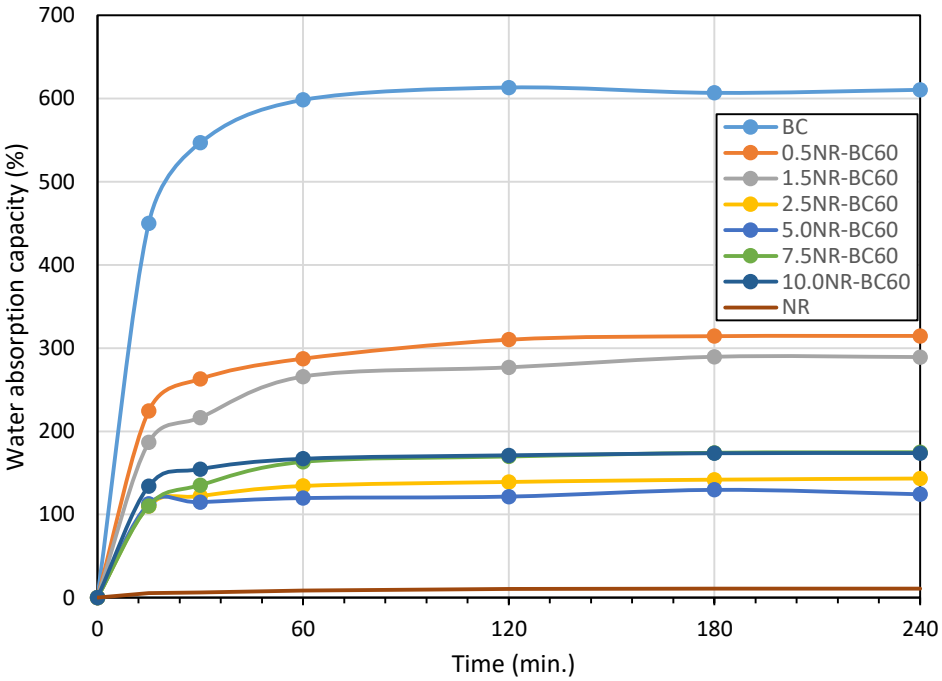

Figure 4. 15 Water absorption capacity of BC and composite films for the immersion temperature at 60 ℃.

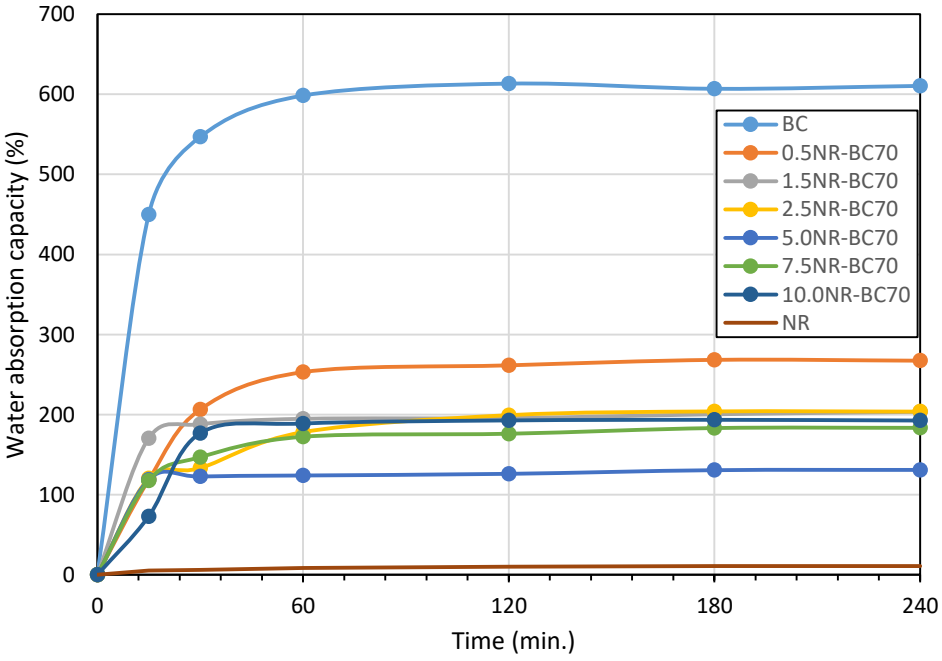

Figure 4. 16 Water absorption capacity of BC and composite films for the immersion temperature at 70 ℃.

The results in Figure 4.13-4.16 show water absorption capacities of BC and composite films during the immersion of samples in distilled water for 4 h. It was observed that the swelling degrees of all samples increased with time. The rapid rate of water adsorption was observed in the first 30 min, and then the rate was slower. The equilibrium absorption was reached at around 1 h. From Table 4.2, pure BC film showed highly water absorption at 610.5% in distilled water because of the hydrophilic functional group of the hydroxyl group (-OH) in its structure [7]. Opposed to pure BC, the water absorption of pure NR was very low at 10.9% because of the hydrophobicity of NR. The water absorption capacities of NR-BC composite films would be in the range of BC and NR films. The effect of NR concentration on the water absorption capacity of composite film was observed. The water absorption capacity of composite films modified by 2.5-5% NRL solution showed the lowest absorbed because the high layer of NR on surface BC film could prevent the penetration of water through the BC film. The water absorption capacity of NR-BC 30 was in the range of 131.2-288.1%. After increasing the immersion temperature to 50°C, 60°C and 70°C, the WACs of composite films were in the range of 88.4-213.9%, 124.3-314.7%, 131.0-267.4%, respectively. The WACs of NR-BC50 and NR-BC60 were relatively low in comparison to the other composite films.

4.1.5 Toluene uptake (TU)

The durable properties are the important properties of composite material. It can be reduced after contact with solvents for a long time because the composite material can dissolve or swell in some solvents, depending on the composition of composite materials. In this research, NR was added into BC film. Generally, NR can easily dissolve in non-polar solutions; and toluene is an aromatic solvent that mostly used in rubber industry. So, the effect of toluene uptake on composites films were investigated by immersing in toluene at room temperature until they were saturated with toluene. The results are shown in Figure 4.17- 4.20 and Table 4.3

Table 4. 3 Toluene uptake (%) of all samples with immersion time 4 h.

Immersion temperature	Toluene uptake (%)							
	BC(0)	0.5	1.5	2.5	5	7.5	10	NR(100)
30	6.44	10.53	13.79	13.86	21.72	9.6	19.24	1075.19
50	6.44	24.12	20.98	49.16	40.16	19.78	28.96	1075.19
60	6.44	23.79	17.88	46.46	39.31	28.26	31.33	1075.19
70	6.44	17.8	14.64	42.98	38.69	28.57	24.32	1075.19

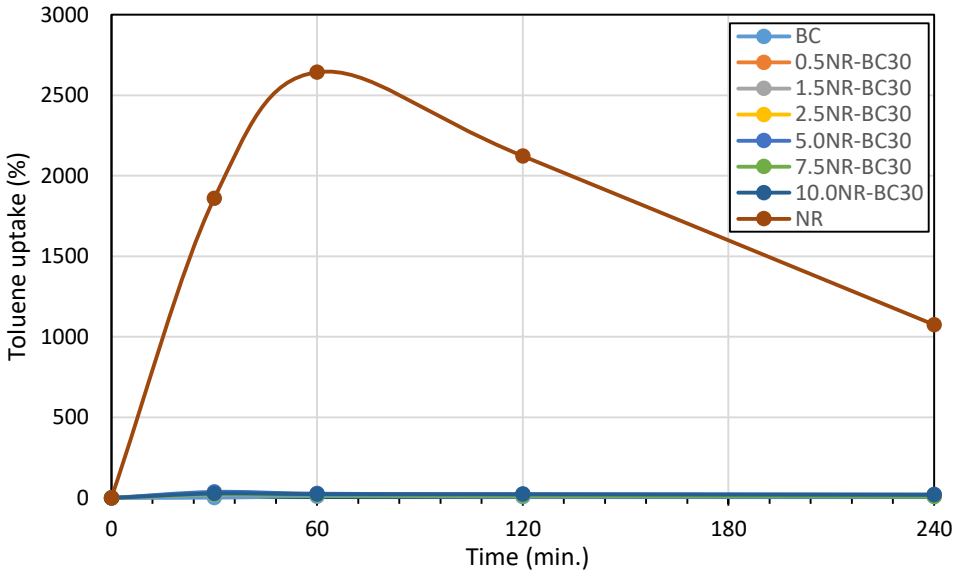

Figure 4. 17 Toluene uptake (%) of BC and composite films of immersion temperature at 30 °C

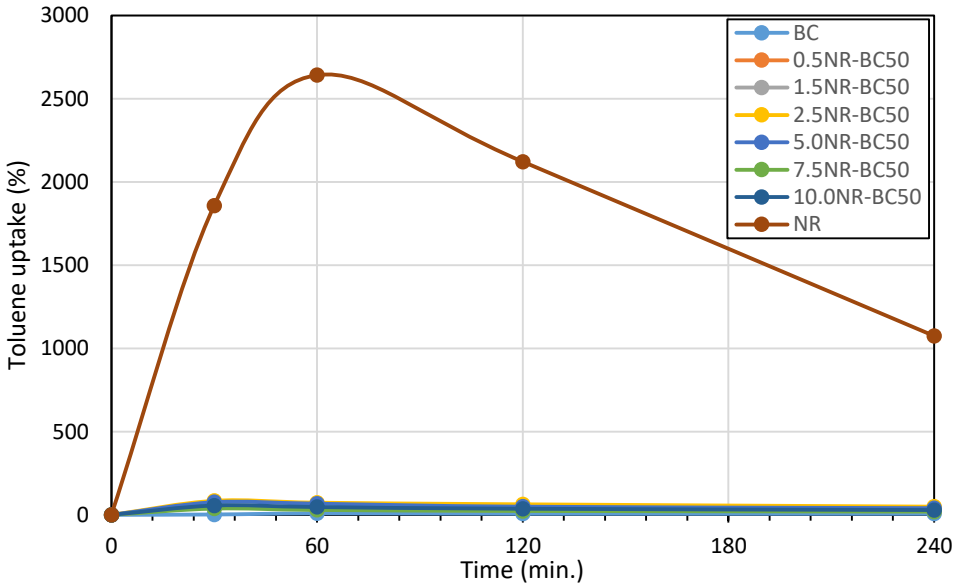

Figure 4. 18 Toluene uptake (%) of BC and composite films of immersion temperature at 50 °C.

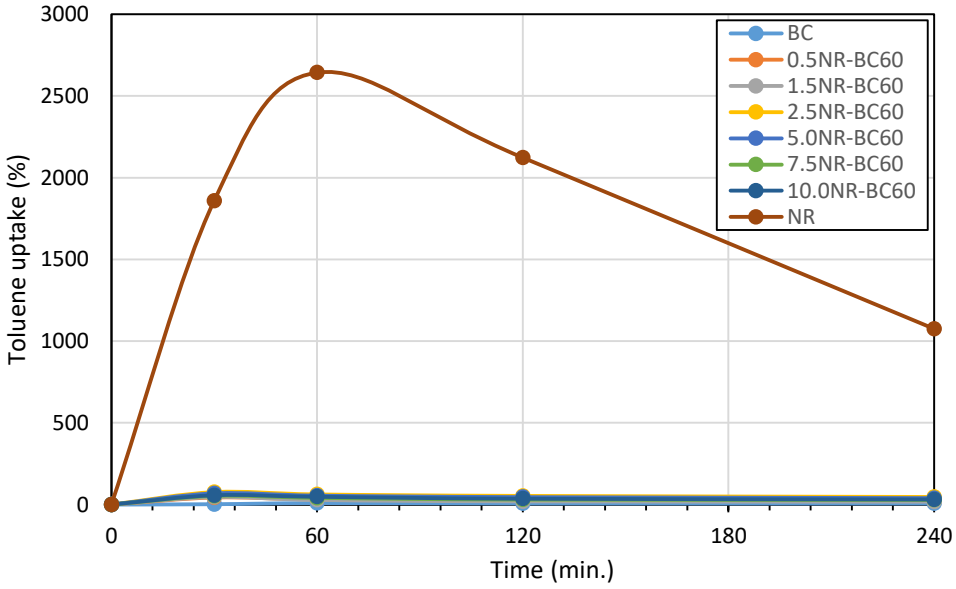

Figure 4. 19 Toluene uptake (%) of BC and composite films of immersion temperature at 60 °C.

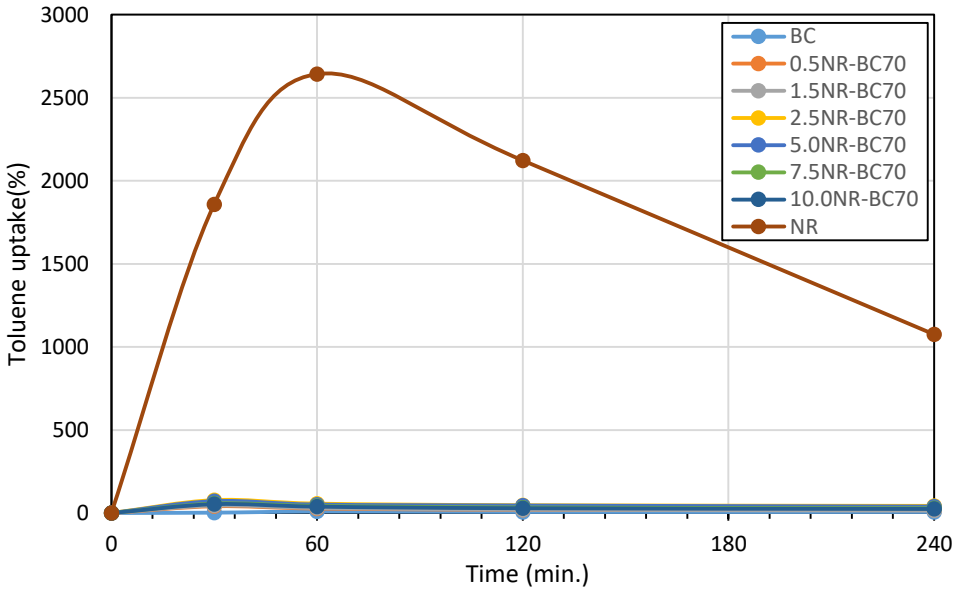

Figure 4. 20 Toluene uptake (%) of BC and composite films of immersion temperature at 70 °C.

At initial absorption, the toluene uptake of NR film rapidly increased and showed the maximum value at 2642% in 1 h. After that, it was decreased when increasing the immersion time due to the dissolution of NR film in toluene [66]. As shown in table 4.3, pure BC film exhibited the lowest toluene uptake at 6.4% because of the hydrophilic nature of BC. The toluene uptakes of composite film were much lower as compared to that of NR film. NR-BC30 films show relatively low toluene uptake, which were in range of 9.6-21.72% at all rubber content. The values of toluene uptake of NR-BC50, NR-BC60 and NR-BC70 were slightly higher, related to the amount of NR inserted into BC surface, which were in the ranges of 19.78-49.16%, 17.88-46.46% and 14.64-42.98% for the immersion temperature at 50°C, 60°C and 70°C, respectively. The modification with NRL solution at the concentration of 2.5 – 5% and immersion temperature of 50°C – 60°C exhibited high value of toluene absorption at approximately 39.31-49.16%. All composite films remained in original shape after the immersion in toluene for 10 hours due to the structural stability of composite films in nonpolar solvent.

4.1.6 X-ray diffraction analysis (XRD)

X-ray diffraction analysis was characterized to know the crystallographic nature of BC and NR-BC composite films. The XRD pattern of BC and NR-BC films shown in Figure 4.21-4.24.

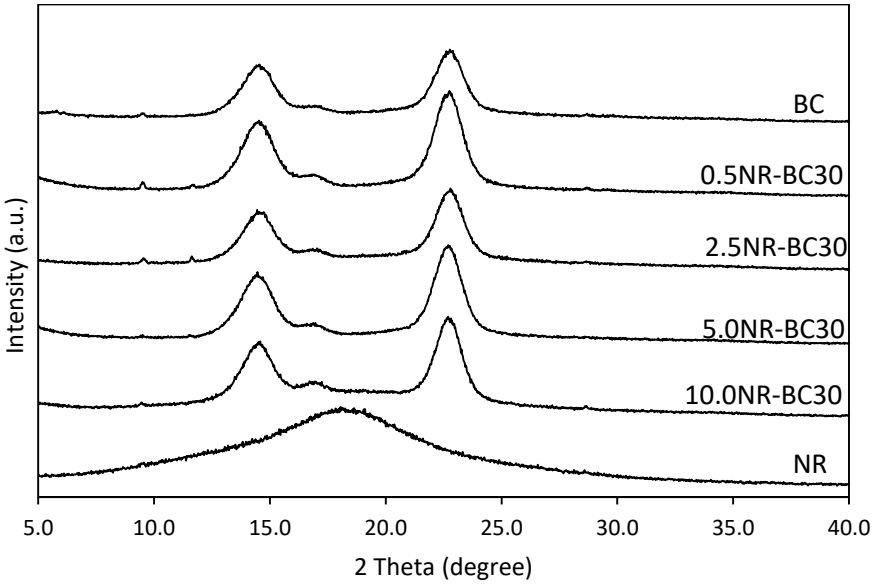

Figure 4. 21 XRD pattern of BC and composite films of immersion temperature at 30 ℃

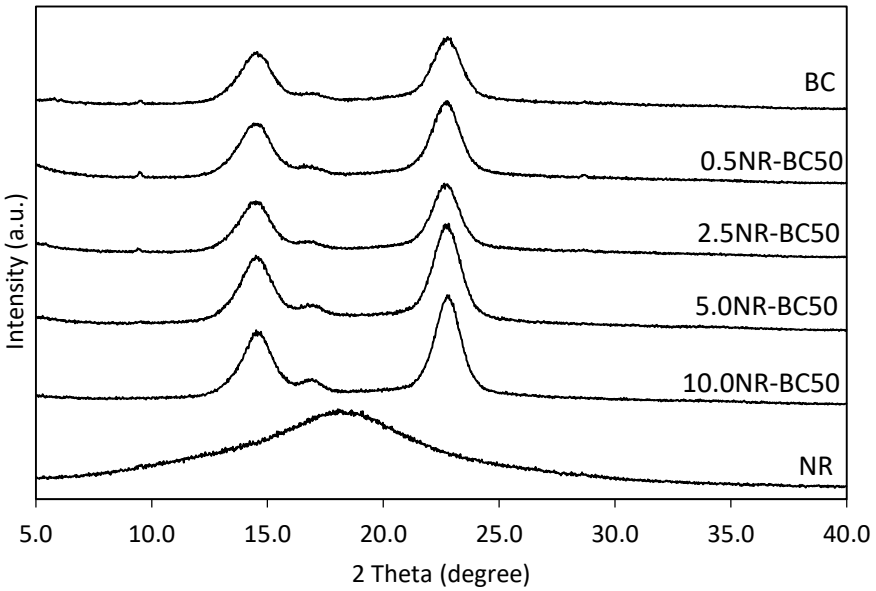

Figure 4. 22 XRD pattern of BC and composite films of immersion temperature at 50 ℃

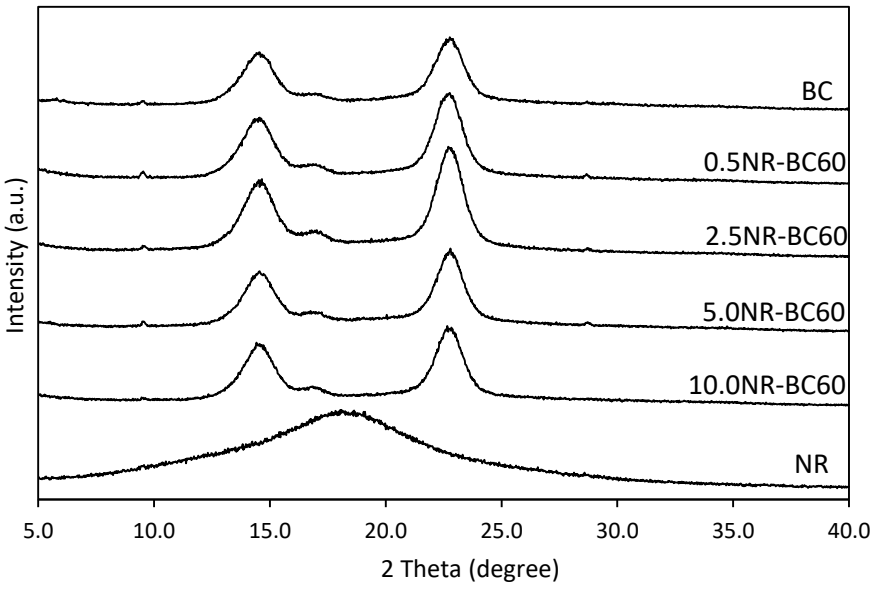

Figure 4. 23 XRD pattern of BC and composite films of immersion temperature at 60 ℃

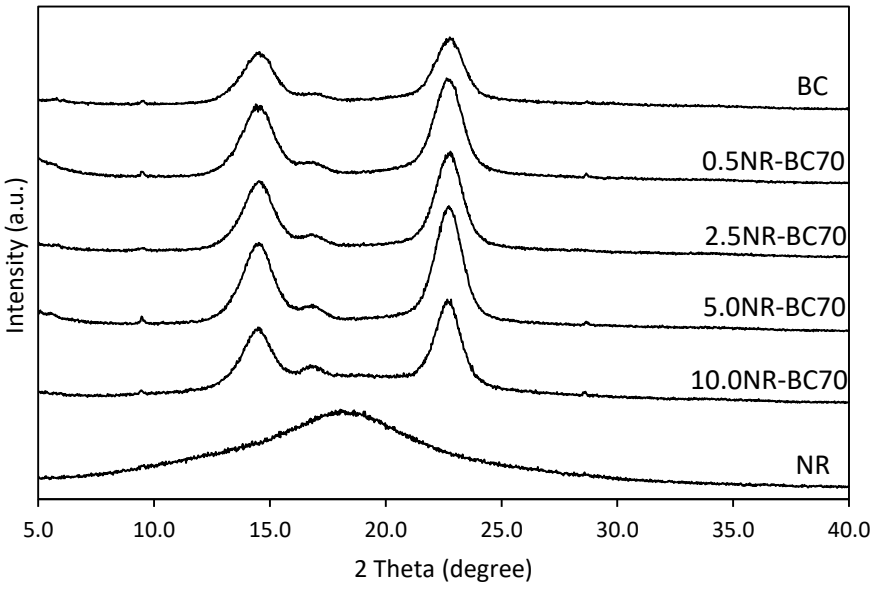

Figure 4. 24 XRD pattern of BC and composite films of immersion temperature at 70 ℃

The characteristic peak of BC consists of three main peaks present at 2 thetas 14.53°, 17° and 22.78° for a crystal plane, which represent a typical profile of cellulose [67]. The diffraction pattern from nanocellulose exhibited a sharp peak indicating that an orderly arrangement of cellulose chain in the crystalline region whereas a broad peak of BC showed the BC is not consisting only crystalline material, a less order

orientation the region of amorphous. NR film displays a typical behavior of an amorphous polymer. The prominent broad hump located around 2 thetas equal to 18°. The composite material at various concentration and immersion temperature shown the same position pattern of the strong BC indicating that the crystalline structure bacterial nanocellulose exists. Due to a small amount of NR, the XRD pattern cannot detect a broad hump of NR. However, the existence of NR in the composite films was clearly observed previously in the cross-section of dry composite films from FESEM micrograph.

4.1.7 Differential Scanning Calorimetry (DSC)

Differential Scanning Calorimetry (DSC) is the thermal analysis used to determine the thermal properties of BC and NR-BC composite films in terms of the glass transition temperature (T_g), melting temperature (T_m) and decomposition temperature (T_d). Not only does the difference degree of polymerization can change the physical properties of composite material, but also on the modification by adding some chemical additive. In this experiment, DSC curves of the BC, NR and NR-BC composite films was measured during the heating range of -100 to 400°C with heating rate 5°C/min, the heat flow measurement for composite films shown in Figure 4.25-4.28. The glass transition temperature (T_g) of pure cellulose was hardly detect in due to the high crystalline structure of nanocellulose exhibited flat heat flow curves and difficult to separate from baseline, According to literature, the glass transition of BC observed at -13°C [68, 69]. In this experiment, the glass transition temperature (T_g) of BC observed at approximately -16°C. The exothermic peak of BC film observed two peaks. The first peak at 217°C indicated the thermal degradation of proteinaceous matter in BC film [52, 70]. the second peak start at approximately 300-340°C indicated the partial pyrolysis of cellulose [71]. Whereas the DSC thermogram of NR exhibited T_g at -62.3°C and T_p observed at 366°C [72]. The DSC thermogram of composite films observed endothermic peak starting at 30°C to 160°C indicating that the dehydration process would break the strongly bond between water and the hydroxyl group of cellulose [52, 73]. The glass transition temperature of NR and BC still occurred at the same range in composite films while the decomposition temperature of composite

films shown in wider range when the comparison with BC film. This indicated that the pyrolysis period increased with increasing amount of NR layer on BC film. However, the DSC thermogram of composite films were slightly appreciable change from those of unmodified BC film.

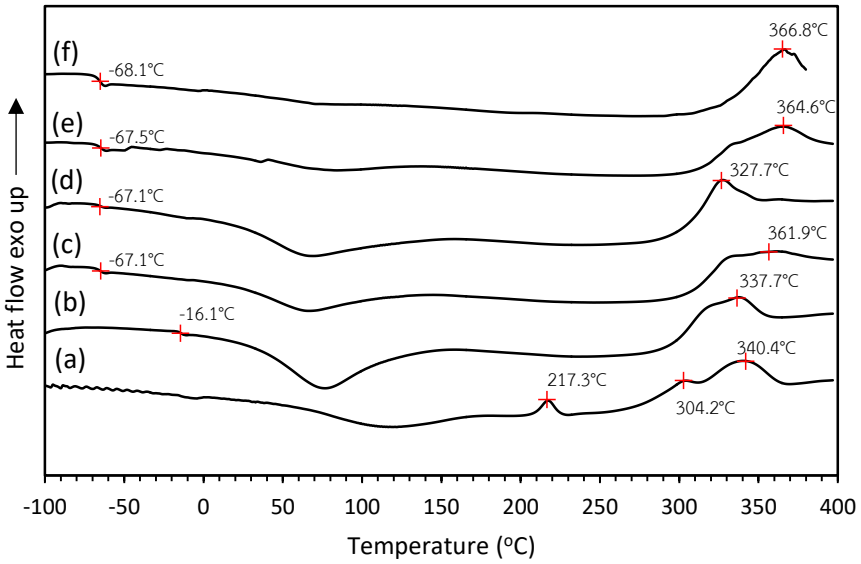

Figure 4. 25 DSC thermograms of BC (a), NR(f) and composite films with 0.5%(b), 2.5%(c), 5%(d) and 10%(e) NR concentration at immersion temperature 30 °C

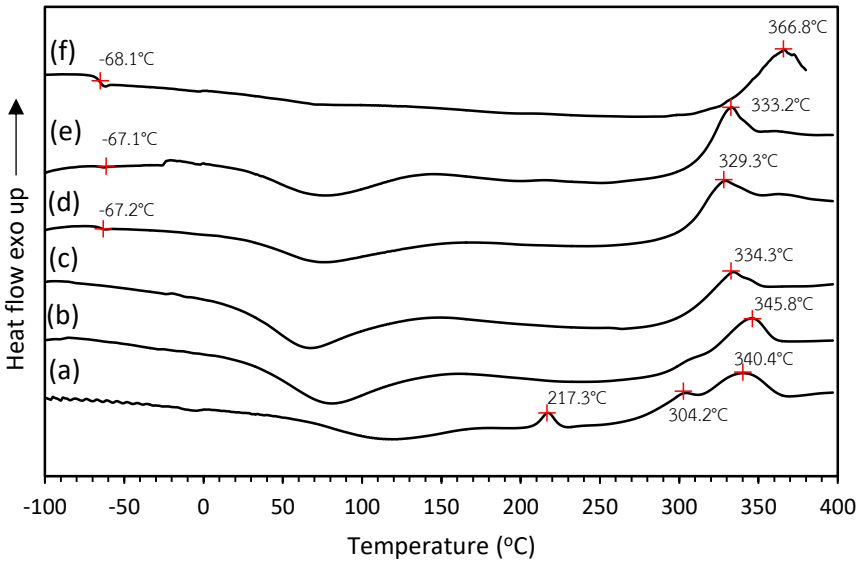

Figure 4. 26 DSC thermograms of BC(a), NR(f) and composite films with 0.5%(b), 2.5%(c), 5%(d) and 10%(e) NR concentration at immersion temperature 50 °C

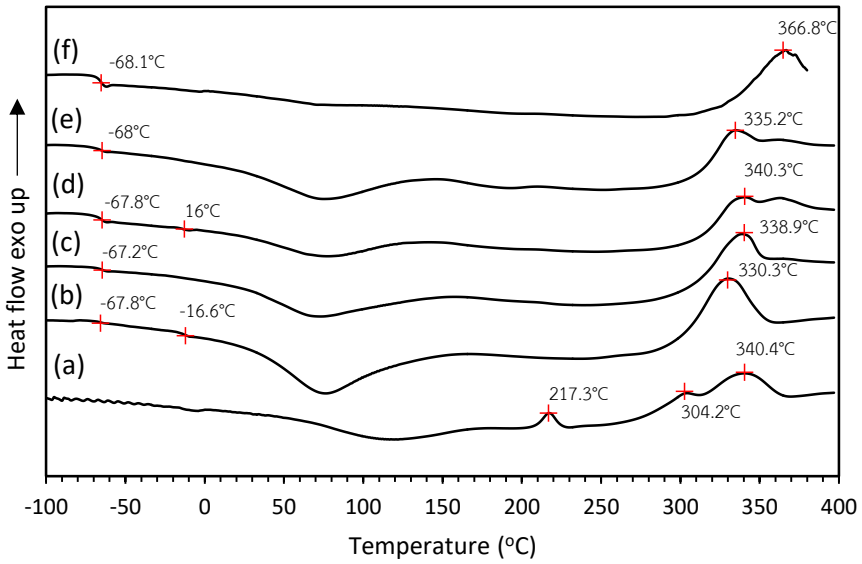

Figure 4. 27 DSC thermograms of of BC(a), NR(f) and composite films with 0.5%(b), 2.5%(c), 5%(d) and 10%(e) NR concentration at immersion temperature 60 °C

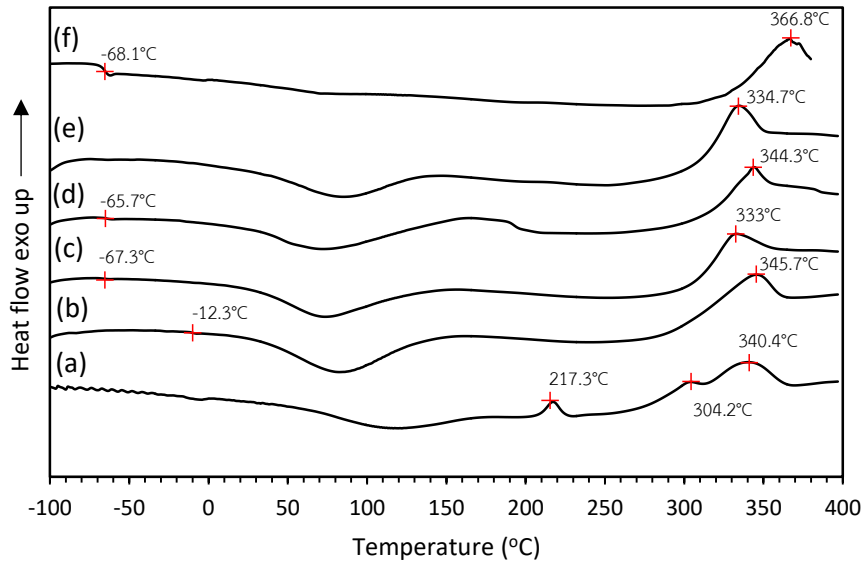

Figure 4. 28 DSC thermograms of of BC(a), NR(f) and composite films with 0.5%(b), 2.5%(c), 5%(d) and 10%(e) NR concentration at immersion temperature 70 °C

4.1.8 Thermal gravimetric analysis (TGA)

Thermal gravimetric analysis (TGA) was used to measure percentage weight of material relation to the increment of temperature. This method provided information about the phase change of material such as dehydration, decomposition and oxidation. There are several factor affect to the TGA curves such as simple gelmetry, compatibility and heating rate [68]. The thermal decomposition of BC started from 30°C to 200°C, which was associated with the vaporization of water [68, 74, 75]. The percentage weight loss of BC shoulder at temperature range 210°C to 240°C was approximately 6% indicating to the decomposition of proteins and nucleic acid [68]. The major pyrolysis of BC was occurred around 300°C to 360°C, which was attributed to the decomposition fo cellulose such as depolymerization and decomposition of glucose units [75]. The percentage weight residue of BC was 20% probably the formation of char residue. Whereas, the pyrolysis temperature of NR occurred around 340°C to 440°C with the maximum pyrolysis temperature at 380°C.

TGA and DTG curves of composite films at immersion temperature 30°C, 50°C, 60°C and 70°C were shown in Figure 4.29-4.30, 4.31-4.32, 4.33-4.34 and 4.35-4.36, respectively. The thermal decompositions of composite films were divided into three weight loss stage. At temperature lower than 200°C corresponding to dehydration of water. The second and third weight loss stage occurred in similar temperature range at 300°C to 400°C. Which the second and third decomposition stages were implied to the incompatibility between BC and NR or heterogeneous distribution of composite films. The maximum pyrolysis of each sample (T_{max}) could consider by a critical thermal decomposition, which it was calculated from the differential TGA curves. The maximum decompositions of composite films were occurred at 340°C and 380°C in accordance with the decomposition of BC and NR, respectively. However, the TGA curve of composite films by using NR concentration 2.5-5% were slightly shift to the right. The results can imply to the thermal stability of composite films were slightly increased. Which it was obviously seen at immersion temperature 60°C.

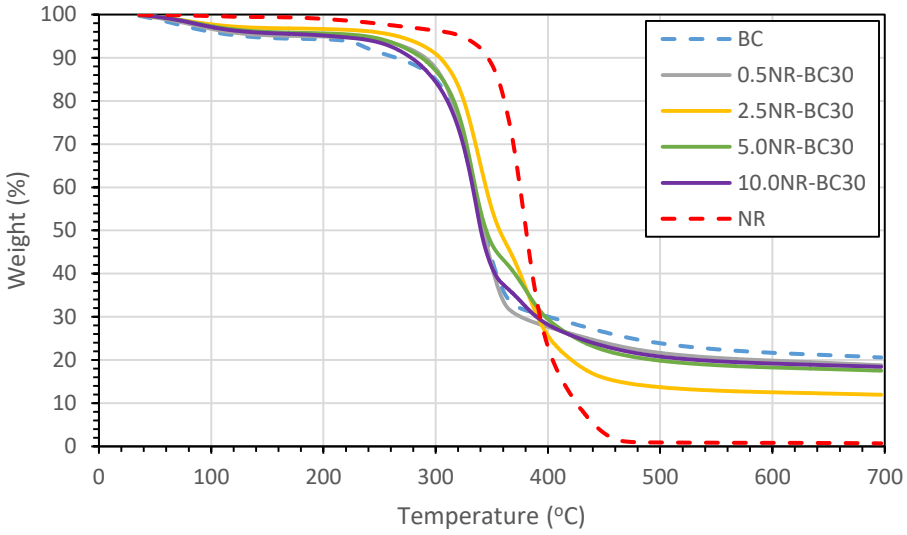

Figure 4. 29 TGA curve of BC, NR, composite films with immersion temperature 30 °C

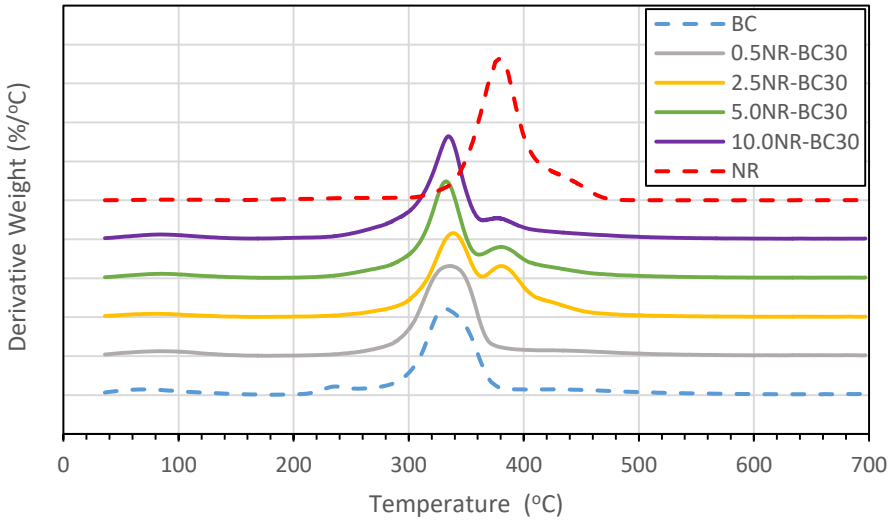

Figure 4. 30 DTG curve of BC, NR, composite films with immersion temperature 30 °C

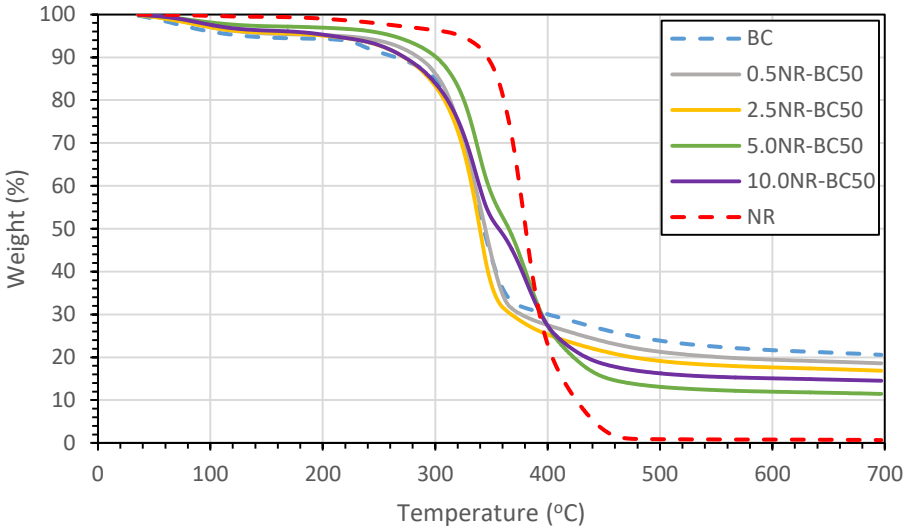

Figure 4. 31 TGA curve of BC, NR, composite films with immersion temperature 50 °C

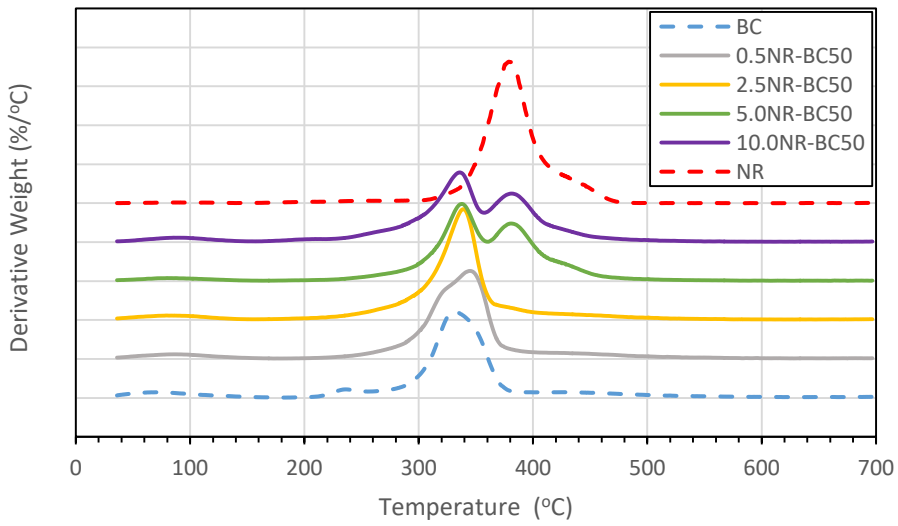

Figure 4. 32 DTG curve of BC, NR, composite films with immersion temperature 50 °C

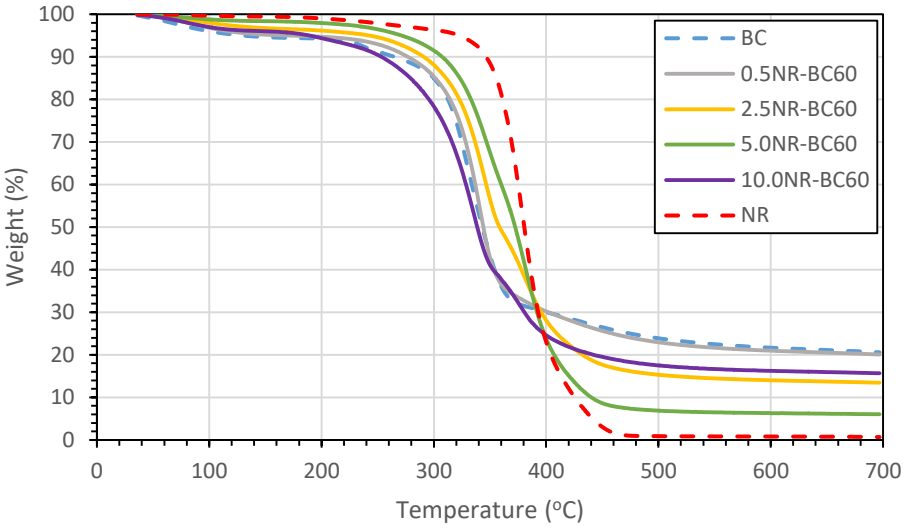

Figure 4. 33 TGA curve of BC, NR, composite films with immersion temperature 60 °C

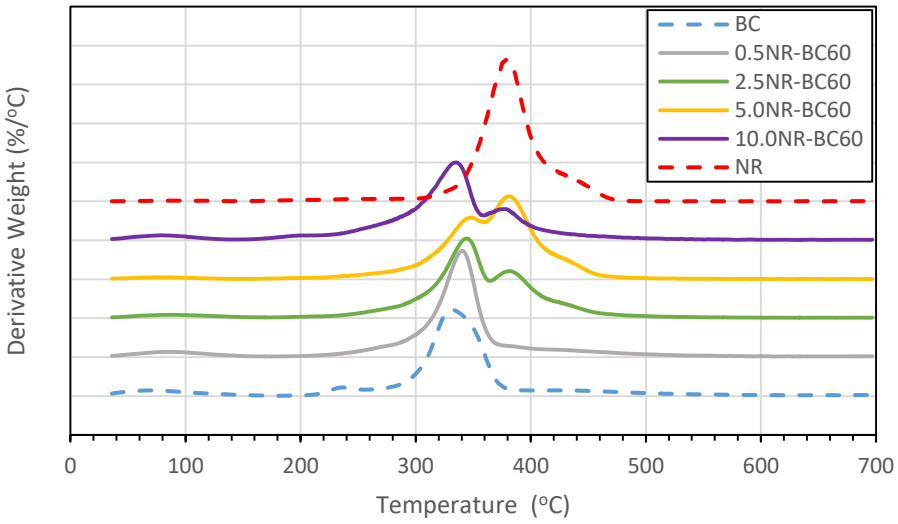

Figure 4. 34 DTG curve of BC, NR, composite films with immersion temperature 60 °C

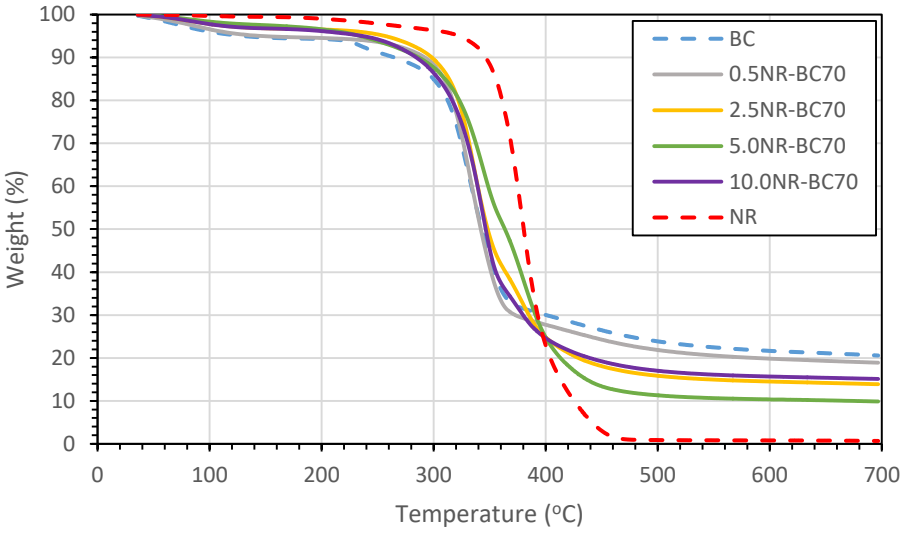

Figure 4. 35 TGA curve of BC, NR, composite films with immersion temperature 70 °C

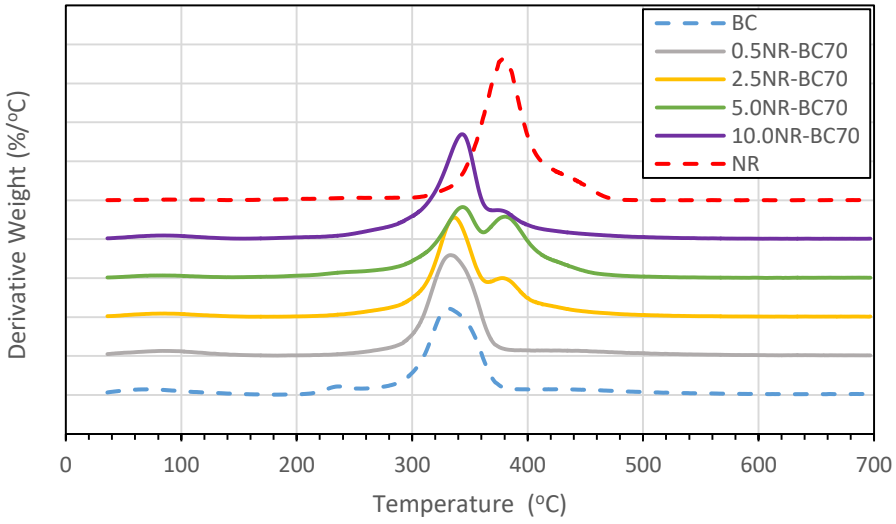

Figure 4. 36 DTG curve of BC, NR, composite films with immersion temperature 70 °C

4.1.9 Mechanical properties

The mechanical properties of BC, NR-BC composite films were analyzed in terms of Young's modulus, tensile strength and elongation at break as shown in Figure 4.16, 4.17 and 4.18, respectively. Because the three-dimensional dense layer of BC the tensile strength showed relatively high. The mechanical of BC exhibited Young's modulus, Tensile strength and elongation at break at 9,135 MPa, 112 MPa and 0.6% as shown in table 4.1; whereas, NR observed at 7.8 MPa, 0.6 MPa and 41.1%, respectively.

Table 4. 4 The mechanical properties of pure BC and NR films

Sample	Young's modulus (MPa)	Tensile strength (MPa)	Elongation at break (%)
BC	9135	112	0.6
NR	7.8	0.6	41.1

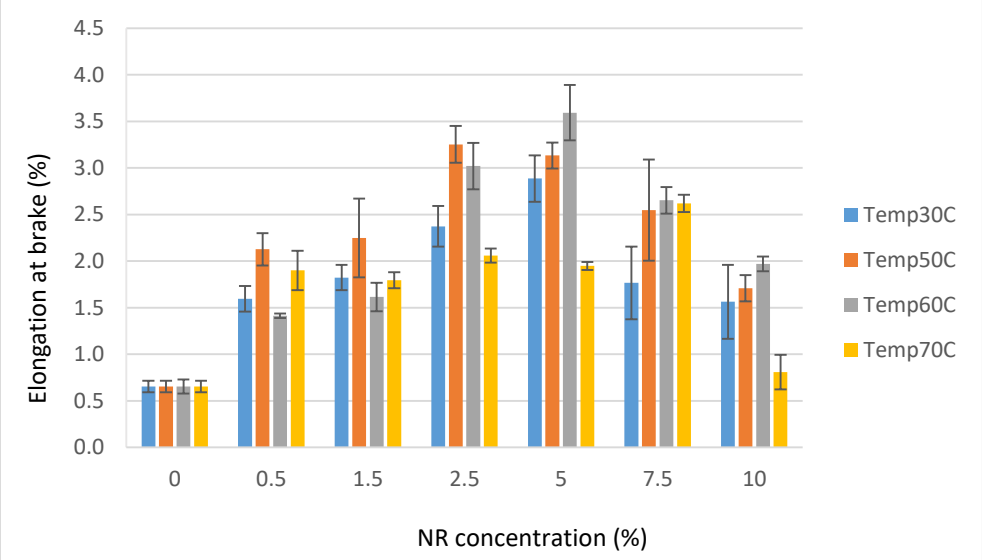

Figure 4. 37 Elongation at break of the dried BC, NR-BC films with various NR concentration and immersion temperature

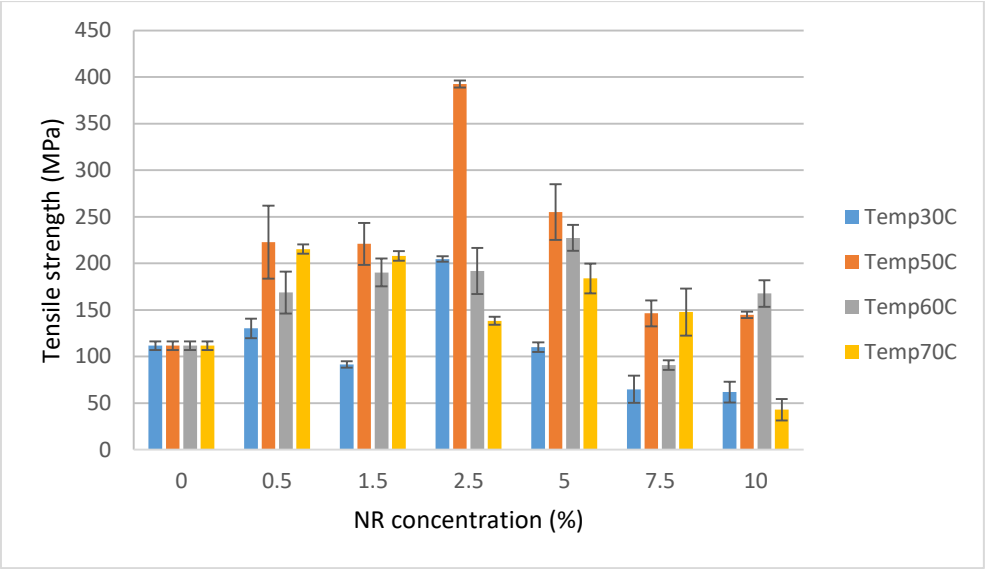

Figure 4. 38 Tensile strength of the dried BC, NR-BC films with various NR concentration and immersion temperature

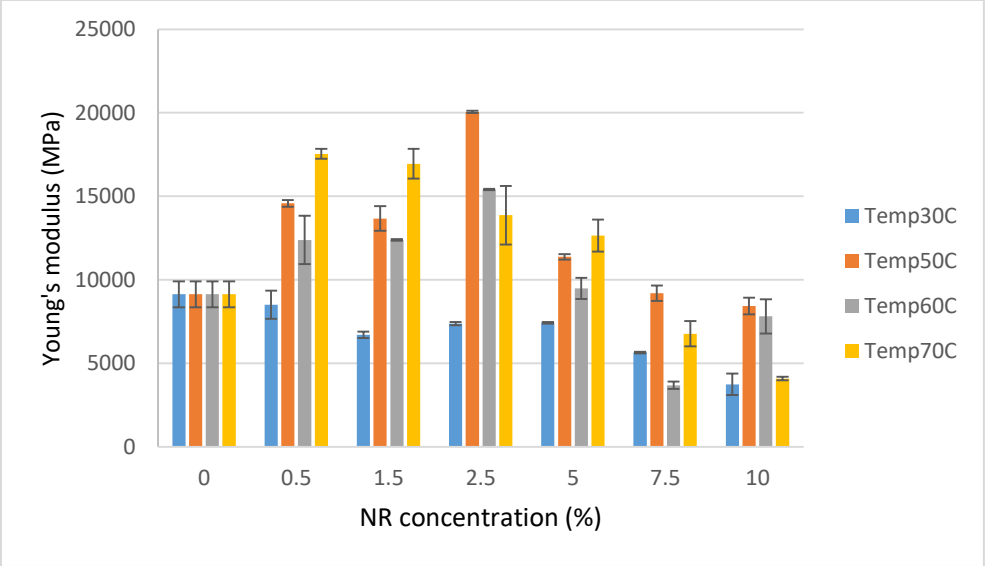

Figure 4. 39 Young's modulus of the dried BC, NR-BC films with various NR concentration and immersion temperature

Percent elongation at break of composite films is shown in Figure 4.37; BC exhibited at 0.65% whereas the composite films had higher elongation at break compared to BC. The elongations at break of the dried NR-BC composite films enhanced with the increment of NR molecules, which depended on concentration of loading NRL solution and immersion temperature. With NR loading by 2.5-5% NRL solution and immersion temperature at 50-60°C, the high value of elongation at break

of the NR-BC composite films in the range of 3.0 - 3.5% was observed which was about 5 – 6 fold as compared to that of normal BC film. At the optimum immersion condition, the dense packed layer of NR in the surface of BC film was clearly observed by SEM analysis. NR molecules were also filled in BC nanofiber networks and between nanocellulose sheets of BC films. This condition resulted in greater ability to absorb the energy to prevent BC cellulose fiber network from breaking and made the composite film more extended before break.

Figure 4.38 shows the tensile strength of BC and composite films, the tensile strength of modified BC films by loading NRL were also significantly higher when compared to the pure BC. The condition for high tensile strength value of composite films was immersion at 2.5% NR concentration with 50°C. In addition, the tensile strength of composite films at 5% NR concentration with immersion temperature around 50-60°C were also high when comparison to pure BC. The force load of 2.5NR-BC50, 2.5NR-BC60, 5NR-BC50 and 5NR-BC60 were 3.5, 1.71, 2.28 and 2.04 fold compared with the unmodified BC, respectively. The reasons for the increment of tensile strength of modified films should be due to the high structural regularity of NR, which tends to crystalline spontaneously when it is stretched [76]. Furthermore, the binds of NR layer on a surface of nanocellulose would restrict the movement of nanocellulose fiber and reinforce both BC and NR to resist the external work load force [77]. Tensile strength of composite films considerable increased due to the high layer of NR on BC surface films. Which it clearly seen in SEM micrograph. The presence of NR within the BC nanocellulose film provided a notable of mechanical properties of the composite films.

Figure 4.39 shows Young's modulus of pure BC and composite films. The results show that Young's modulus of BC exhibited at 9135 MPa, whereas the composite films show higher Young's modulus when compared with pure BC. At 2.5% NR concentration with immersion temperature at 50°C, the highest Young's modulus in this research was obtained to approximately 20,000 MPa. When the NR concentration more than 5%, the Young's modulus decreased with increasing NR concentrations and immersion temperature. This enhancement of tensile strength and Young's modulus was influenced by the synergistic of NR and BC nanocellulose matrix.

The mechanical properties data of all samples were shown in Appendix D (Table D.2) and the supplement mechanical data of composite films for 5% and 10% immersion with 60°C without ethanol were also show in table D.1.

4.1.10 Biodegradation in soil

Biodegradability is the one of the essential properties for environmental issues. This property is important for the application of the composite materials such as for packaging. From previous discussion, BC structures consist of an orderly arrangement in term of crystalline nanocellulose fibers and a small amount of non-orderly cellulose chain called amorphous cellulose. In this structure was conveniently attacked by enzymatic degradation. Some previous literature reported that the characteristics of cellulose biodegradation behavior consist of two major step process. In the first step, *Endoglucanases* (endo-1,4-β-glu-canases,EGs) would hydrolyze amorphous regions of the cellulose fibers while the reducing and non-reducing ends were attacked by *Cellobiohydrolases* (exo-1,4-β-glucanases, CBHs), CBHs were efficiently enzyme that degrades crystalline cellulose. The results of cellulose degradation from both enzymes would releases cellobiose molecules. In the second step, the cellobiose molecules were broken down and release two glucose molecule by $\beta-$glucosidases [78, 79] Whereas the conformation of NR is relatively resistant to microorganisms biodegradation compared with many other natural polymers [80]. The general type of microorganism of NR biodegradation was found in soil such as *Bacillus* sp.

In this research, the biodegradability of BC and composite films was examined in soil burial treatment under uncontrolled composting conditions. The sample of each NR concentration with immersion temperature at 30°C and 50°C were checked for the weight residue weekly for 6 weeks. The percent weight losses of BC and composite films as a function of biodegradation time are shown in Table 4.5.

Table 4. 5 The percent weight loss of BC and composite films with immersion temperature at 30°C and 50°C as a function of biodegradation time

Samples	Weight loss (%)						
	Time (Weeks)						
	0	1	2	3	4	5	6
BC	0	21.1	54.97	75.31	100	-	-
0.5NR-BC30	0	19.31	36.83	65.67	100	-	-
2.5NR-BC30	0	11.84	25.37	54.35	89.48	100	-
5NR-BC30	0	13.39	29.01	60.39	100	-	-
10NR-BC30	0	13.93	37.97	62.41	100	-	-
0.5NR-BC50	0	16.34	37.35	59.57	100	-	-
2.5NR-BC50	0	10.34	21.9	49.53	82.84	92.42	100
5NR-BC50	0	11.57	29.2	54.6	88.02	100	-
10NR-BC50	0	12.79	44.64	58.11	100	-	-

From Table 4.5, the results show that BC film had weight loss percentage higher than other films and was completely decomposed in 4 weeks after embed in soil. The composite films with various concentrations of NRL loading and immersion temperatures were decomposed around 4 - 5 weeks depend on the thickness of NR layer under a surface of BC. The comparison of composite films between the immersion at 30°C and 50°C showed the higher of weight loss of the composite films immersion with 30°C, which indicated the higher rate of decomposition. In addition, the slowest rate of decomposition for this research was observed by 2.5% NRL loading concentration. The difference weight loss of BC and NR-BC composite film depend on the resistance to microorganism attacks between BC and NR. At the same time, NR and BC were attacked by the different microorganism. For BC, the microorganism would attack to amorphous region of nanocellulose first, after that it would decompose all crystalline regions. On the other hand, the degradation of isoprene structure of NRL was a slow process [81]. The remaining composite films after the test showed loose structure, high stretch and became lumpy due to the decomposition of nanocellulose

by microorganism, while some NR on the surface of BC still exist, which indicated that NR had slower rate of decomposition by microorganism than nanocellulose of BC [56].

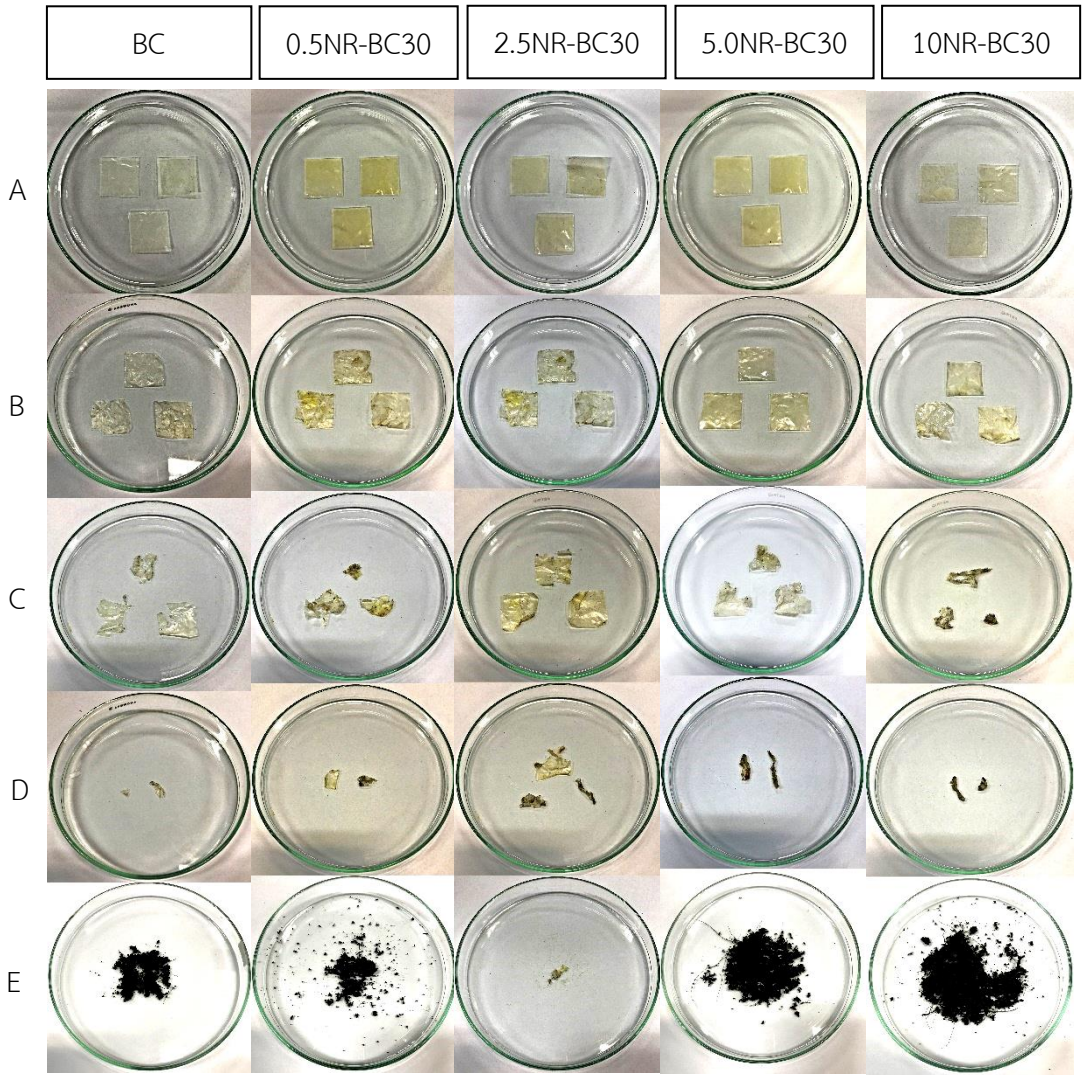

Figure 4. 40 The samples of BC and composite films with immersion temperature at 30°C after testing in soil for 0(A), 1(B), 2(C), 3(D) and 4(E) weeks.

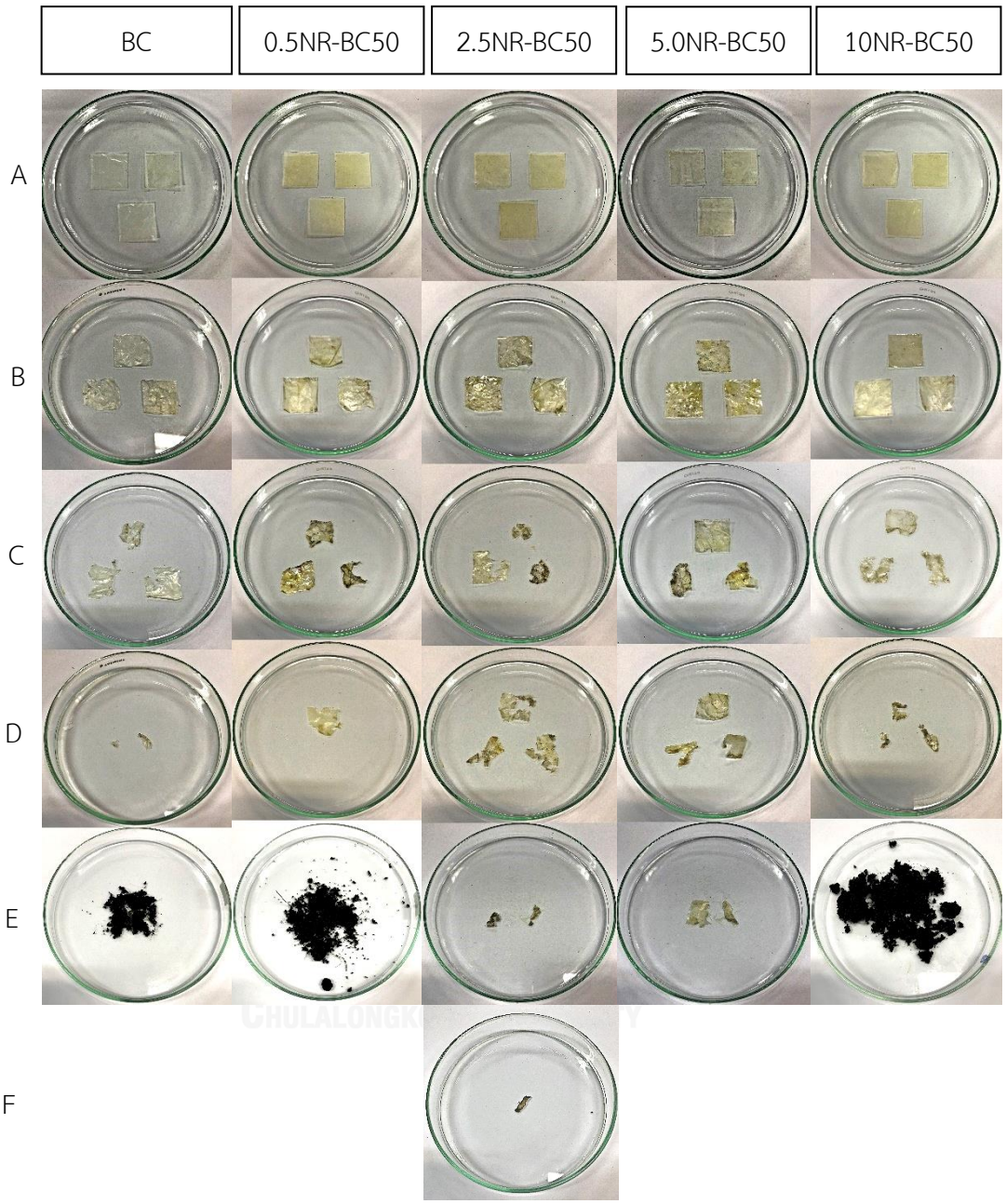

Figure 4. 41 The samples of BC and composite films with immersion temperature at 50°C after testing in soil for 0(A), 1(B), 2(C), 3(D), 4(E) and 5(F) weeks.

CHAPTER 5

CONCLUSIONS

The modification of bacterial cellulose films by immersing BC membrane into 0.5-10% NRL solution at the immersion temperature of 30-70°C with the addition of 50% (v/v) ethanol for the viscosity reduction were investigated. The optimum conditions for the immersion were as follows: NRL concentration of 2.5-5%, immersion temperature of 50-60°C. This conditions show high thickness of NR-BC composite films, which significantly promoted the outstanding mechanical properties of the film. The synergism of BC and NR composite prepared at NRL concentration of 2.5% and immersion temperature 50°C show the highest mechanical properties at 392.43 MPa, 3.25% and 20051.3 MPa for tensile strength, elongation at break and Young's modulus, respectively. The composite films demonstrated structural stability in both polar and nonpolar solvents (water and toluene). Weak physical interaction between BC and NR was observed by FTIR analysis. The crystallinity structure of the composite films remained as BC structure including the thermal properties of the composite films which were analyzed by XRD and DSC. From TGA results, the thermal stability of composite films slightly increased with wider range of pyrolysis period. Finally, the results of biodrgradation in soil showed the composite films could completely degrade for 5-6 weeks. The decomposition rate depends on the thickness of NR layer in the BC surface.

REFERENCES

[1] Shoda, M. and Sugano, Y. Recent advances in bacterial cellulose production. Biotechnology and Bioprocess Engineering 10(1) (2005): 1.

[2] Fontana, J., et al. Acetobacter cellulose pellicle as a temporary skin substitute. Applied Biochemistry and Biotechnology 24(1) (1990): 253-264.

[3] Ougiya, H., Watanabe, K., Morinaga, Y., and Yoshinaga, F. Emulsion-stabilizing effect of bacterial cellulose. Bioscience, biotechnology, and biochemistry 61(9) (1997): 1541-1545.

[4] Klemm, D., Schumann, D., Udhardt, U., and Marsch, S. Bacterial synthesized cellulose—artificial blood vessels for microsurgery. Progress in Polymer Science 26(9) (2001): 1561-1603.

[5] Svensson, A., et al. Bacterial cellulose as a potential scaffold for tissue engineering of cartilage. Biomaterials 26(4) (2005): 419-431.

[6] Millon, L. and Wan, W. The polyvinyl alcohol–bacterial cellulose system as a new nanocomposite for biomedical applications. Journal of Biomedical Materials Research Part B: Applied Biomaterials 79(2) (2006): 245-253.

[7] Lin, W.-C., Lien, C.-C., Yeh, H.-J., Yu, C.-M., and Hsu, S.-h. Bacterial cellulose and bacterial cellulose–chitosan membranes for wound dressing applications. Carbohydrate polymers 94(1) (2013): 603-611.

[8] Feng, C., et al. Flexible, stretchable, transparent conducting films made from superaligned carbon nanotubes. Advanced Functional Materials 20(6) (2010): 885-891.

[9] Jacob, M., Thomas, S., and Varughese, K.T. Mechanical properties of sisal/oil palm hybrid fiber reinforced natural rubber composites. Composites Science and Technology 64(7) (2004): 955-965.

[10] BHATTACHARYYA, T.B., Biswas, A.K., Chatterjee, J., and Pramanick, D. Short pineapple leaf fibre reinforced rubber composites. Plastics and rubber processing and applications 6(2) (1986): 119-125.

[11] Arumugam, N., Selvy, K.T., Rao, K.V., and Rajalingam, P. Coconut-fiber-reinforced rubber composites. Journal of applied polymer science 37(9) (1989): 2645-2659.

[12] Ismail, H., Edyham, M., and Wirjosentono, B. Bamboo fibre filled natural rubber composites: the effects of filler loading and bonding agent. Polymer testing 21(2) (2002): 139-144.

[13] De, D., De, D., and Adhikari, B. Curing characteristics and mechanical properties of alkali-treated grass-fiber-filled natural rubber composites and effects of bonding agent. Journal of applied polymer science 101(5) (2006): 3151-3160.

[14] Klemm, D., Heublein, B., Fink, H.P., and Bohn, A. Cellulose: fascinating biopolymer and sustainable raw material. Angewandte Chemie International Edition 44(22) (2005): 3358-3393.

[15] Wei, L. and McDonald, A.G. A review on grafting of biofibers for biocomposites. Materials 9(4) (2016): 303.

[16] Jonas, R. and Farah, L.F. Production and application of microbial cellulose. Polymer Degradation and Stability 59(1-3) (1998): 101-106.

[17] Iguchi, M., Yamanaka, S., and Budhiono, A. Bacterial cellulose—a masterpiece of nature's arts. Journal of Materials Science 35(2) (2000): 261-270.

[18] Saibuatong, O.-a. and Phisalaphong, M. Novo aloe vera–bacterial cellulose composite film from biosynthesis. Carbohydrate polymers 79(2) (2010): 455-460.

[19] Wan, Y., et al. Synthesis and characterization of hydroxyapatite–bacterial cellulose nanocomposites. Composites Science and Technology 66(11) (2006): 1825-1832.

[20] Gea, S., Bilotti, E., Reynolds, C., Soykeabkeaw, N., and Peijs, T. Bacterial cellulose–poly (vinyl alcohol) nanocomposites prepared by an in-situ process. Materials Letters 64(8) (2010): 901-904.

[21] Yamanaka, S., et al. The structure and mechanical properties of sheets prepared from bacterial cellulose. Journal of Materials Science 24(9) (1989): 3141-3145.

[22] Eichhorn, S.J., et al. Review: current international research into cellulose nanofibres and nanocomposites. Journal of Materials Science 45(1) (2010): 1.

[23] Hsieh, Y.-C., Yano, H., Nogi, M., and Eichhorn, S. An estimation of the Young's modulus of bacterial cellulose filaments. Cellulose 15(4) (2008): 507-513.

[24] Chawla, P.R., Bajaj, I.B., Survase, S.A., and Singhal, R.S. Microbial cellulose: fermentative production and applications. Food Technology and Biotechnology 47(2) (2009): 107-124.

[25] Bielecki, S., Krystynowicz, A., Turkiewicz, M., and Kalinowska, H. Bacterial cellulose. Biopolymers online (2005).

[26] Quero, F. Interfacial micromechanics of bacterial cellulose bio-composites using Raman spectroscopy. (2012).

[27] Phowan, P. and Tantatrian, S. Production of cellulose by Acetobacter xylinum at high temperature. (2011).

[28] Masaoka, S., Ohe, T., and Sakota, N. Production of cellulose from glucose by Acetobacter xylinum. Journal of fermentation and bioengineering 75(1) (1993): 18-22.

[29] Hestrin, S. and Schramm, M. Synthesis of cellulose by Acetobacter xylinum. 2. Preparation of freeze-dried cells capable of polymerizing glucose to cellulose. Biochemical Journal 58(2) (1954): 345.

[30] Watanabe, K., Tabuchi, M., Morinaga, Y., and Yoshinaga, F. Structural features and properties of bacterial cellulose produced in agitated culture. Cellulose 5(3) (1998): 187-200.

[31] Dudman, W. Cellulose production by Acetobacter strains in submerged culture. Microbiology 22(1) (1960): 25-39.

[32] Dick, J.S. Rubber technology: compounding and testing for performance. Carl Hanser Verlag GmbH Co KG, 2014.

[33] Nimpaiboon, A., Amnuaypornsri, S., and Sakdapipanich, J.T. OBSTRUCTION OF STORAGE HARDENING IN NR BY USING POLAR CHEMICALS. Rubber Chemistry and Technology 89(2) (2016): 358-368.

[34] Nawamawat, K., Sakdapipanich, J.T., Ho, C.C., Ma, Y., Song, J., and Vancso, J.G. Surface nanostructure of Hevea brasiliensis natural rubber latex particles.

Colloids and Surfaces A: Physicochemical and Engineering Aspects 390(1) (2011): 157-166.

[35] Orphardt, C.E. Denaturation of Proteins. Virtual Chembook, Elmhurst College 3 (2003).

[36] Bowler, W.W. Electrophoretic mobility study of fresh Hevea latex. Industrial & Engineering Chemistry 45(8) (1953): 1790-1794.

[37] Subramaniam, A. Gel permeation chromatography of natural rubber. Rubber Chemistry and Technology 45(1) (1972): 346-358.

[38] Kovuttikulrangsie, S. and Tanaka, Y. NR latex particle size and its molecular weight from young and mature hevea trees. Journal of Rubber Research 2(3) (1999): 150-159.

[39] Ohya, N., Tanaka, Y., and Koyama, T. Activity of rubber transferase and rubber particle size in Hevea latex. Journal of Rubber Research 3(4) (2000): 214-221.

[40] Sakdapipanich, J.T., Suksujaritporn, S., and Tanaka, Y. Structural characterisation of the small rubber particles in fresh Hevea latex. Journal of Rubber Research 2(3) (1999): 160-168.

[41] Sakdapipanich, J.T. and Rojruthai, P. Molecular structure of natural rubber and its characteristics based on recent evidence. Biotechnology-Molecular Studies and Novel Applications for Improved Quality of Human Life 213 (2012).

[42] Lide, D.R. CRC handbook of chemistry and physics. 12J204 (1947).

[43] Bodhibukkana, C., et al. Composite membrane of bacterially-derived cellulose and molecularly imprinted polymer for use as a transdermal enantioselective controlled-release system of racemic propranolol. Journal of Controlled Release 113(1) (2006): 43-56.

[44] Trovatti, E., et al. Bacterial cellulose membranes applied in topical and transdermal delivery of lidocaine hydrochloride and ibuprofen: in vitro diffusion studies. International Journal of Pharmaceutics 435(1) (2012): 83-87.

[45] Suedee, R., Bodhibukkana, C., Tangthong, N., Amnuaikit, C., Kaewnopparat, S., and Srichana, T. Development of a reservoir-type transdermal enantioselective-controlled delivery system for racemic propranolol using a

molecularly imprinted polymer composite membrane. Journal of Controlled Release 129(3) (2008): 170-178.

[46] Maneerung, T., Tokura, S., and Rujiravanit, R. Impregnation of silver nanoparticles into bacterial cellulose for antimicrobial wound dressing. Carbohydrate polymers 72(1) (2008): 43-51.

[47] kingkaew, J. and Phisalaphong, M. development of bacterial cellulose nanocomposite film for medical application. (2011).

[48] Cai, Z. and Kim, J. Bacterial cellulose/poly (ethylene glycol) composite: characterization and first evaluation of biocompatibility. Cellulose 17(1) (2010): 83-91.

[49] Leitão, A.F., Silva, J.P., Dourado, F., and Gama, M. Production and characterization of a new bacterial cellulose/poly (vinyl alcohol) nanocomposite. Materials 6(5) (2013): 1956-1966.

[50] Jewprasat, S. and Phisalaphong, M. pervaporation of ethanol water mixtures using bacterial cellulose-poly(vinyl alcohol) membrane. (2014).

[51] Taokaew, S., Nunkaew, N., Siripong, P., and Phisalaphong, M. Characteristics and anticancer properties of bacterial cellulose films containing ethanolic extract of mangosteen peel. Journal of Biomaterials Science, Polymer Edition 25(9) (2014): 907-922.

[52] Suratago, T., Taokaew, S., Kanjanamosit, N., Kanjanaprapakul, K., Burapatana, V., and Phisalaphong, M. Development of bacterial cellulose/alginate nanocomposite membrane for separation of ethanol–water mixtures. Journal of Industrial and Engineering Chemistry 32 (2015): 305-312.

[53] Rungjang, W. and Sukyai, P. Bacterial cellulose filled natural rubber composites.pdf. (2013).

[54] Trovatti, E., Capote, T.S., and Scarel-Caminaga, R.M. DEVELOPMENT AND CHARACTERIZATION OF NATURAL RUBBER AND BACTERIAL CELLULOSE-SPONGE COMPOSITES. (2015).

[55] Tarachiwin, L., Sakdapipanich, J., Ute, K., Kitayama, T., and Tanaka, Y. Structural characterization of α-terminal group of natural rubber. 2.

Decomposition of branch-points by phospholipase and chemical treatments. Biomacromolecules 6(4) (2005): 1858-1863.

[56] Tangpakdee, J. and Tanaka, Y. Characterization of sol and gel in Hevea natural rubber. Rubber Chemistry and Technology 70(5) (1997): 707-713.

[57] van Koningsveld, G.A., et al. Effects of ethanol on structure and solubility of potato proteins and the effects of its presence during the preparation of a protein isolate. Journal of agricultural and food chemistry 50(10) (2002): 2947-2956.

[58] Roberts, R. and Briggs, D. Characteristics of various soybean globulin components with respect to denaturation by ethanol. Cereal Chemistry 40(4) (1963): 450-&.

[59] Wolf, W., Eldridge, A., and Babcock, G. Physical properties of alcohol-extracted soybean proteins. Cereal Chemistry 40(5) (1963): 504-&.

[60] Chaikumpollert, O., Yamamoto, Y., Suchiva, K., and Kawahara, S. Protein-free natural rubber. Colloid and Polymer Science 290(4) (2012): 331-338.

[61] Kawahara, S., Kakubo, T., Nishiyama, N., Tanaka, Y., Isono, Y., and Sakdapipanich, J.T. Crystallization behavior and strength of natural rubber: Skim rubber, deproteinized natural rubber, and pale crepe. Journal of applied polymer science 78(8) (2000): 1510-1516.

[62] Phomrak, S. and Phisalaphong, M. Reinforcement of Natural Rubber with Bacterial Cellulose via a Latex Aqueous Microdispersion Process. Journal of Nanomaterials 2017 (2017).

[63] Halib, N., Amin, M.C.I.M., and Ahmad, I. Physicochemical properties and characterization of nata de coco from local food industries as a source of cellulose (Sifat fizikokimia dan pencirian nata de coco daripada industri makanan tempatan sebagai sumber selulosa). Sains Malaysiana 41(2) (2012): 205-211.

[64] Guidelli, E.J., Ramos, A.P., Zaniquelli, M.E.D., and Baffa, O. Green synthesis of colloidal silver nanoparticles using natural rubber latex extracted from Hevea brasiliensis. Spectrochimica Acta Part A: Molecular and Biomolecular Spectroscopy 82(1) (2011): 140-145.

[65] Păvăloiu, R.-D., Stoica-Guzun, A., and Dobre, T. Swelling studies of composite hydrogels based on bacterial cellulose and gelatin. UPB Sci. Bull. Ser. B 77(1) (2015): 53-62.

[66] Obasi, H.C., Ogbobe, O., and Igwe, I.O. Diffusion characteristics of toluene into natural rubber/linear low density polyethylene blends. International journal of polymer science 2009 (2010).

[67] Czaja, W., Romanovicz, D., and Malcolm Brown, R. Structural investigations of microbial cellulose produced in stationary and agitated culture. Cellulose 11(3-4) (2004): 403-411.

[68] George, J., Ramana, K.V., Sabapathy, S.N., Jagannath, J.H., and Bawa, A.S. Characterization of chemically treated bacterial (Acetobacter xylinum) biopolymer: Some thermo-mechanical properties. International journal of biological macromolecules 37(4) (2005): 189-194.

[69] Baranov, A., Anisimova, V., and Khripunov, A. Glass transition and dielectric properties of acetobacter xylinum cellulose. 2005.

[70] Brown, E.E. and Laborie, M.-P.G. Bioengineering bacterial cellulose/poly (ethylene oxide) nanocomposites. Biomacromolecules 8(10) (2007): 3074-3081.

[71] Barud, H., et al. Thermal characterization of bacterial cellulose–phosphate composite membranes. Journal of Thermal Analysis and Calorimetry 87(3) (2007): 815-818.

[72] Burfield, D.R. and Lim, K.L. Differential scanning calorimetry analysis of natural rubber and related polyisoprenes. Measurement of the glass transition temperature. Macromolecules 16(7) (1983): 1170-1175.

[73] Oliveira, R.L., et al. Synthesis and characterization of methylcellulose produced from bacterial cellulose under heterogeneous condition. Journal of the Brazilian Chemical Society 26(9) (2015): 1861-1870.

[74] Nata, I.F., Sureshkumar, M., and Lee, C.-K. One-pot preparation of amine-rich magnetite/bacterial cellulose nanocomposite and its application for arsenate removal. Rsc Advances 1(4) (2011): 625-631.

[75] Barud, H.S., et al. Thermal behavior of cellulose acetate produced from homogeneous acetylation of bacterial cellulose. Thermochimica Acta 471(1) (2008): 61-69.

[76] Arayapranee, W. Rubber abrasion resistance. in Abrasion Resistance of Materials: InTech, 2012.

[77] Ahmad, M.R., Ahmad, N.A., Suhaimi, S.A., Bakar, N.A.A., Ahmad, W.Y.W., and Salleh, J. Tensile and tearing strength of uncoated and natural rubber latex coated high strength woven fabrics. in Humanities, Science and Engineering Research (SHUSER), 2012 IEEE Symposium on, pp. 541-545: IEEE, 2012.

[78] Pérez, J., Munoz-Dorado, J., de la Rubia, T., and Martinez, J. Biodegradation and biological treatments of cellulose, hemicellulose and lignin: an overview. International Microbiology 5(2) (2002): 53-63.

[79] Béguin, P. and Aubert, J.-P. The biological degradation of cellulose. FEMS microbiology reviews 13(1) (1994): 25-58.

[80] Cherian, E. and Jayachandran, K. Microbial Degradation of Natural Rubber Latex by a novel Species of Bacillus sp. SBS25 isolated from Soil. (2010).

[81] Rose, K. and Steinbüchel, A. Biodegradation of natural rubber and related compounds: recent insights into a hardly understood catabolic capability of microorganisms. Applied and Environmental Microbiology 71(6) (2005): 2803-2812.

APPENDIX

APPENDIX A. THE COMPOSITE FILMS FROM IMMERSION METHOD.

1. Morphology of composite films with immersion temperature 50°C.

0.5NR-BC50 1.5NR-BC50 2.5NR-BC50 5.0NR-BC50 7.5NR-BC50 10NR-BC50

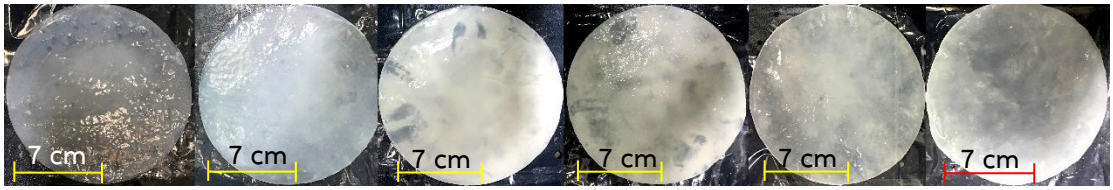

Figure A. 1 Never-dried composite films of NR concentration at 0.5, 1.5, 2.5, 5, 7.5 and 10% v/v immersion at 50°C

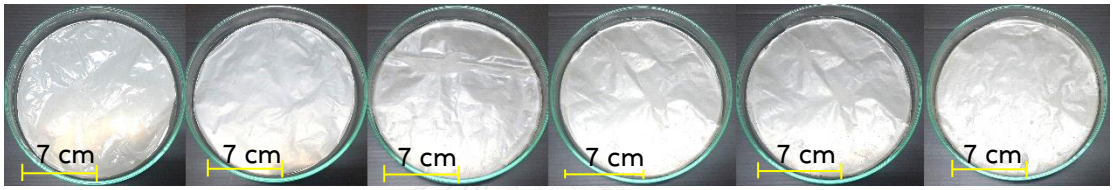

Figure A. 2 dried composite films of NR concentration at 0.5, 1.5, 2.5, 5, 7.5 and 10% v/v immersion at 50°C

2. Preliminary test of ethanol concentration in NR latex.

2 ml. of 50%v/v ethanol 2.5 ml. of 50%v/v ethanol 3 ml. of 50%v/v ethanol

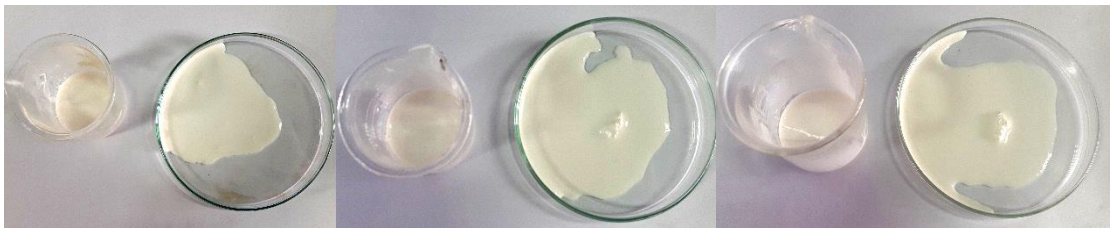

Figure A. 3 the ratio of ethanol concentration in 100 ml of rubber solution and the NR agglomeration at room temperature.

Table A. 1 The concentration of 60% drc NRL using in the immersion process by total amount of volume of NR dispersion 300 ml and adding with 6 ml of 50% (v/v) ethanol.

NR concentration (%v/v)	Volume of 60%drcNRL (ml.)	Volume of water (ml.)
0.5	2.5	297.5
2.5	25	275
5	12.5	287.5
7.5	37.5	262.5
10	50	250

3. The dried weight data of composite films

Table A. 2 The dried weight data of composite films

Samples	Average dried weight[(a)] (g)	Samples	Average dried weight[(a)] (g)
BC	0.0091		
0.5NR-BC30	0.0096	0.5NR-BC60	0.0103
1.5NR-BC30	0.0094	1.5NR-BC60	0.0117
2.5NR-BC30	0.0115	2.5NR-BC60	0.0158
5.0NR-BC30	0.0095	5.0NR-BC60	0.0155
7.5NR-BC30	0.0094	7.5NR-BC60	0.0116
10.0NR-BC30	0.0096	10.0NR-BC60	0.0101
0.5NR-BC50	0.0101	0.5NR-BC70	0.0093
1.5NR-BC50	0.0097	1.5NR-BC70	0.0097
2.5NR-BC50	0.014	2.5NR-BC70	0.012
5.0NR-BC50	0.013	5.0NR-BC70	0.0121
7.5NR-BC50	0.0117	7.5NR-BC70	0.0112
10.0NR-BC50	0.0108	10.0NR-BC70	0.0099

[(a)] Value are average of 3 specimens

APPENDIX B. THE WATER ABSORPTION CAPACITY DATA.

Table B. 1 The dried (W_d) and hydrated (W_h) weight data of BC, NR and NR-BC30 films

samples	specimen	W_h (g)						
		Time (min)						
		W_d (g) 0	15	30	60	120	180	240
BC	1	0.0084	0.0432	0.0478	0.0536	0.0545	0.0539	0.0558
	2	0.0074	0.0332	0.0392	0.0409	0.0441	0.0419	0.0412
	3	0.009	0.06	0.0734	0.0787	0.0783	0.0795	0.0792
	average	0.008	0.045	0.053	0.058	0.059	0.058	0.059
NR	1	0.0939	0.0953	0.0963	0.0982	0.1	0.1002	0.1003
	2	0.101	0.111	0.111	0.1139	0.1153	0.1163	0.1163
	3	0.12	0.126	0.127	0.1296	0.132	0.1328	0.1328
	Average	0.105	0.111	0.111	0.114	0.116	0.116	0.116
0.5NR-BC30	1	0.0085	0.0197	0.0207	0.0225	0.0218	0.0242	0.026
	2	0.0083	0.0204	0.0206	0.0237	0.0259	0.025	0.0251
	3	0.0085	0.0209	0.0216	0.024	0.025	0.0256	0.0264
	average	0.008	0.020	0.021	0.023	0.024	0.025	0.026
1.5NR-BC30	1	0.0107	0.0208	0.0221	0.0266	0.023	0.0248	0.025
	2	0.0128	0.0239	0.0227	0.0253	0.0235	0.0269	0.028
	3	0.0121	0.0261	0.0255	0.0279	0.0263	0.0269	0.0293
	average	0.012	0.024	0.023	0.027	0.024	0.026	0.027
2.5NR-BC30	1	0.0096	0.0223	0.023	0.0267	0.0303	0.0288	0.0273
	2	0.012	0.0275	0.0246	0.0282	0.0265	0.0341	0.0359
	3	0.0111	0.0231	0.0258	0.0234	0.0259	0.0266	0.0251
	average	0.011	0.024	0.024	0.026	0.028	0.030	0.029
5NR-BC30	1	0.015	0.031	0.0368	0.0363	0.0307	0.0389	0.04
	2	0.0097	0.0243	0.025	0.028	0.0293	0.0297	0.0285
	3	0.0128	0.0338	0.0369	0.0393	0.0376	0.04	0.0392
	average	0.013	0.030	0.033	0.035	0.033	0.036	0.036
7.5NR-BC30	1	0.0103	0.0546	0.063	0.0735	0.0856	0.0832	0.0833
	2	0.0093	0.032	0.0358	0.0424	0.0436	0.044	0.0423
	3	0.0089	0.0276	0.0293	0.0349	0.035	0.0373	0.035
	average	0.010	0.038	0.043	0.050	0.055	0.055	0.054
10NR-BC30	1	0.0115	0.0347	0.0363	0.0437	0.0453	0.044	0.046
	2	0.016	0.0305	0.0317	0.0344	0.0355	0.0364	0.0355
	3	0.0106	0.0306	0.0458	0.054	0.0571	0.0551	0.055
	average	0.013	0.032	0.038	0.044	0.046	0.045	0.046

Table B. 2 The dried (W_d) and hydrated (W_h) weight data of BC, NR and NR-BC50 and NR-BC60 films.

samples	specimen	W_h (g)						
		Time (min)						
		W_d (g) 0	15	30	60	120	180	240
0.5NR-BC50	1	0.0082	0.0168	0.0181	0.0186	0.0182	0.0189	0.0187
	2	0.0072	0.0252	0.0229	0.0299	0.0306	0.0333	0.0323
	3	0.0083	0.0202	0.0203	0.0234	0.0237	0.024	0.0234
	Average	0.008	0.021	0.020	0.024	0.024	0.025	0.025
1.5NR-BC50	1	0.008	0.0185	0.0208	0.0214	0.0215	0.0215	0.0215
	2	0.0089	0.0232	0.0262	0.0273	0.0274	0.0275	0.0272
	3	0.0075	0.0212	0.0218	0.0253	0.0253	0.0266	0.0265
	Average	0.008	0.021	0.023	0.025	0.025	0.025	0.025
2.5NR-BC50	1	0.0113	0.0201	0.0202	0.0212	0.0214	0.0222	0.0226
	2	0.013	0.0216	0.022	0.0232	0.023	0.025	0.0245
	3	0.0163	0.0276	0.0287	0.0299	0.0296	0.0299	0.0294
	Average	0.014	0.023	0.024	0.025	0.025	0.026	0.026
5NR-BC50	1	0.0117	0.0208	0.0209	0.0212	0.0214	0.0224	0.0222
	2	0.0111	0.019	0.0203	0.0208	0.0203	0.0209	0.0204
	3	0.0114	0.0195	0.0201	0.0214	0.0216	0.0214	0.0219
	Average	0.011	0.020	0.020	0.021	0.021	0.022	0.022
7.5NR-BC50	1	0.0113	0.0229	0.0226	0.0235	0.0234	0.0246	0.0241
	2	0.011	0.0206	0.0212	0.0229	0.023	0.023	0.0233
	3	0.0085	0.0166	0.0172	0.018	0.018	0.019	0.0191
	Average	0.010	0.020	0.020	0.021	0.021	0.022	0.022
10NR-BC50	1	0.0091	0.0194	0.0202	0.0225	0.0229	0.0228	0.0225
	2	0.0084	0.0197	0.0209	0.0212	0.0216	0.0217	0.0215
	3	0.0086	0.017	0.0173	0.018	0.0195	0.0194	0.0193
	Average	0.009	0.019	0.019	0.021	0.021	0.021	0.021
0.5NR-BC60	1	0.0112	0.0382	0.0452	0.0459	0.052	0.0526	0.0528
	2	0.01	0.0297	0.032	0.034	0.0348	0.0348	0.0346
	3	0.0095	0.0317	0.0342	0.039	0.0391	0.0398	0.0399
	Average	0.010	0.033	0.037	0.040	0.042	0.042	0.042
1.5NR-BC60	1	0.0095	0.0259	0.0283	0.0337	0.0342	0.037	0.0367
	2	0.0097	0.0269	0.0301	0.0338	0.0349	0.0351	0.035
	3	0.0106	0.0326	0.0359	0.0415	0.0432	0.044	0.0443
	Average	0.0099	0.0285	0.0314	0.0363	0.0374	0.0387	0.0387

Table B. 3 The dried (W_d) and hydrated (W_h) weight data of BC, NR and NR-BC60 and NR-BC70 films.

samples	specimen	Wh (g)						
		Time (min)						
		Wd (g) 0	15	30	60	120	180	240
2.5NR-BC60	1	0.0097	0.0316	0.0344	0.0367	0.0379	0.0381	0.0384
	2	0.014	0.0147	0.016	0.0182	0.0187	0.0189	0.0191
	3	0.0198	0.0451	0.0462	0.047	0.0474	0.0482	0.0483
	Average	0.015	0.03	0.036	0.034	0.035	0.035	0.035
5NR-BC60	1	0.0095	0.0189	0.0196	0.0199	0.0199	0.021	0.0201
	2	0.0097	0.0215	0.0204	0.0213	0.0216	0.022	0.0212
	3	0.0092	0.02	0.021	0.0212	0.0214	0.0222	0.0224
	Average	0.009	0.020	0.020	0.021	0.021	0.022	0.021
7.5NR-BC60	1	0.0154	0.0338	0.0354	0.0401	0.0399	0.0401	0.041
	2	0.0188	0.0368	0.0429	0.049	0.0512	0.0517	0.0518
	3	0.0123	0.0272	0.0311	0.0333	0.0343	0.0357	0.035
	Average	0.016	0.033	0.036	0.041	0.042	0.043	0.043
10NR-BC60	1	0.0136	0.0377	0.0414	0.0423	0.0423	0.0424	0.0426
	2	0.018	0.0362	0.0399	0.0438	0.0446	0.0452	0.045
	3	0.0165	0.0387	0.0411	0.0423	0.0435	0.044	0.0441
	Average	0.016	0.038	0.041	0.043	0.043	0.044	0.044
0.5NR-BC70	1	0.0116	0.0231	0.0258	0.0285	0.0294	0.0295	0.0295
	2	0.0091	0.0281	0.0341	0.0403	0.0415	0.0415	0.0415
	3	0.0087	0.0237	0.0302	0.035	0.0354	0.0373	0.037
	Average	0.010	0.025	0.030	0.035	0.035	0.036	0.036
1.5NR-BC70	1	0.0093	0.0359	0.0455	0.048	0.0493	0.0458	0.0468
	2	0.0095	0.0364	0.0441	0.052	0.0524	0.0523	0.0524
	3	0.0094	0.0378	0.0415	0.0518	0.054	0.0564	0.0564
	Average	0.009	0.037	0.044	0.051	0.052	0.052	0.052
2.5NR-BC70	1	0.0153	0.0363	0.0389	0.045	0.0483	0.0496	0.0486
	2	0.017	0.0366	0.0361	0.0446	0.0467	0.0465	0.0475
	3	0.0125	0.0259	0.0295	0.035	0.0391	0.0401	0.04
	Average	0.015	0.033	0.035	0.042	0.045	0.045	0.045
5NR-BC70	1	0.0113	0.0403	0.05	0.05	0.055	0.0556	0.055
	2	0.0118	0.0441	0.045	0.0535	0.0575	0.0571	0.0581
	3	0.0121	0.0442	0.05	0.0591	0.0602	0.062	0.0612
	Average	0.012	0.043	0.048	0.054	0.058	0.058	0.058

Table B. 4 The dried (W_d) and hydrated (W_h) weight data of BC, NR and NR-BC70 films

samples	specimen	Wh (g)						
		Time (min)						
		Wd (g) 0	15	30	60	120	180	240
7.5NR-BC70	1	0.023	0.0415	0.0567	0.0585	0.0606	0.0615	0.0612
	2	0.0302	0.0847	0.067	0.08	0.0805	0.085	0.0855
	3	0.0214	0.0363	0.0605	0.0647	0.0649	0.0648	0.0648
	Average	0.025	0.054	0.061	0.068	0.069	0.070	0.071
10NR-BC70	1	0.022	0.0362	0.0652	0.0673	0.0699	0.0694	0.0695
	2	0.0217	0.0393	0.0548	0.0603	0.0599	0.0608	0.06
	3	0.0213	0.037	0.0599	0.0602	0.0605	0.0606	0.0607
	Average	0.022	0.038	0.060	0.063	0.063	0.064	0.063

Table B. 5 Data for Figure 4.13

Time (min)	Water absorption capacity (%)							
	NR-BC Concentration (%)							
	BC(0)	0.5	1.5	2.5	5	7.5	10	NR(100)
0	0.00	0.00	0.00	0.00	0.00	0.00	0.00	0.00
15	450.00	141.11	98.88	122.94	137.60	151.44	270.53	5.53
30	546.77	148.62	97.47	124.46	163.20	198.69	290.88	6.16
60	598.39	177.47	124.16	139.45	176.27	246.72	316.84	8.51
120	613.31	187.35	104.49	152.91	160.27	261.94	300.70	10.29
180	606.85	195.65	120.79	173.70	189.60	255.64	301.75	10.92
240	610.48	206.32	131.18	170.03	187.20	258.27	288.07	10.92

Table B. 6 Data for Figure 4.14

Time (min)	Water absorption capacity (%)							
	NR-BC Concentration (%)							
	BC(0)	0.5	1.5	2.5	5	7.5	10	NR(100)
0	0.00	0.00	0.00	0.00	0.00	0.00	0.00	0.00
15	450.00	162.45	157.79	70.69	73.39	95.13	114.94	5.53
30	546.77	158.65	181.97	74.63	79.24	98.05	123.75	6.16
60	598.39	203.38	203.28	83.00	85.38	109.09	136.40	8.51
120	613.31	205.91	204.10	82.27	85.09	109.09	145.21	10.29
180	606.85	221.52	209.84	89.90	89.18	116.23	144.83	10.92
240	610.48	213.92	208.20	88.42	88.60	115.91	142.53	10.92

Table B. 7 Data for Figure 4.15

Time (min)	Water absorption capacity (%)							
	NR-BC Concentration (%)							
	BC(0)	0.5	1.5	2.5	5	7.5	10	NR(100)
0	0.00	0.00	0.00	0.00	0.00	0.00	0.00	0.00
15	450.00	224.43	186.58	110.11	112.68	110.32	134.10	5.53
30	546.77	262.87	216.44	122.07	114.79	135.27	154.47	6.16
60	598.39	287.30	265.77	134.25	119.72	163.23	166.94	8.51
120	613.31	310.10	276.85	139.08	121.48	169.68	171.10	10.29
180	606.85	314.33	289.60	141.84	129.58	174.19	173.60	10.92
240	610.48	314.66	289.26	143.22	124.30	174.84	173.80	10.92

Table B. 8 Data for Figure 4.16

Time (min)	Water absorption capacity (%)							
	NR-BC Concentration (%)							
	BC(0)	0.5	1.5	2.5	5	7.5	10	NR(100)
0	0.00	0.00	0.00	0.00	0.00	0.00	0.00	0.00
15	450.00	118.64	170.56	120.54	118.80	117.83	73.08	5.53
30	546.77	206.46	187.88	133.26	122.75	146.92	176.77	6.16
60	598.39	253.06	194.81	178.13	124.01	172.39	188.92	8.51
120	613.31	261.56	195.67	199.33	126.07	176.14	192.77	10.29
180	606.85	268.37	200.43	204.02	130.65	183.24	193.54	10.92
240	610.48	267.35	203.46	203.79	130.96	183.51	192.62	10.92

APPENDIX C. THE TOLUENE UPTAKE DATA.

Table C. 1 The weight of dried specimen before swelling (W_0) and after immersion in toluene (W_t) of BC, NR and NR-BC30 films

samples	specimen	W_t (g)				
		Time (min)				
		W_0 (g) 0	30	60	120	180
BC	1	0.008	0.0077	0.0087	0.0092	0.0092
	2	0.009	0.0095	0.0099	0.009	0.009
	3	0.0094	0.0098	0.0101	0.0099	0.0099
	average	0.009	0.009	0.010	0.009	0.009
NR	1	0.0987	2.067	3.125	2.8871	0.8489
	2	0.0813	1.7578	2.1374	1.7763	1.1572
	3	0.1166	1.9848	2.8721	1.9289	1.4795
	Average	0.099	1.937	2.712	2.197	1.162
0.5NR-BC30	1	0.0085	0.0094	0.0107	0.0099	0.0091
	2	0.0079	0.0089	0.0089	0.0089	0.009
	3	0.0083	0.0115	0.0099	0.0097	0.0092
	average	0.008	0.010	0.010	0.010	0.009
1.5NR-BC30	1	0.0105	0.0143	0.0134	0.0121	0.0111
	2	0.0082	0.0102	0.0094	0.0096	0.0098
	3	0.0103	0.0103	0.0115	0.0121	0.0121
	average	0.010	0.012	0.011	0.011	0.011
2.5NR-BC30	1	0.0121	0.0176	0.0164	0.0145	0.0134
	2	0.011	0.0129	0.0127	0.0121	0.0118
	3	0.0108	0.0143	0.0132	0.0135	0.0134
	average	0.011	0.015	0.014	0.013	0.013
5NR-BC30	1	0.0103	0.014	0.0132	0.0121	0.012
	2	0.0089	0.012	0.0102	0.0099	0.0098
	3	0.0098	0.0139	0.0133	0.0138	0.0135
	average	0.010	0.013	0.012	0.012	0.012
7.5NR-BC30	1	0.0101	0.0127	0.0121	0.0117	0.0114
	2	0.0102	0.0121	0.0112	0.011	0.0099
	3	0.0099	0.0123	0.012	0.0118	0.0118
	average	0.010	0.012	0.012	0.012	0.011
10NR-BC30	1	0.0109	0.0126	0.0121	0.0132	0.0115
	2	0.0129	0.0166	0.0165	0.0156	0.0165
	3	0.0131	0.018	0.017	0.0164	0.016
	average	0.012	0.016	0.015	0.015	0.015

Table C. 2 The weight of dried specimen before swelling (W_0) and after immersion in toluene (W_t) of BC, NR and NR-BC50 and NR-BC60 films

samples	specimen	W_t (g)				
		Time (min)				
		W_0 (g) 0	30	60	120	240
0.5NR-BC50	1	0.0107	0.0131	0.0123	0.0121	0.012
	2	0.0109	0.0176	0.0161	0.0154	0.0142
	3	0.0095	0.0156	0.013	0.013	0.0124
	Average	0.010	0.015	0.014	0.014	0.013
1.5NR-BC50	1	0.0099	0.0112	0.0113	0.011	0.0109
	2	0.0111	0.0131	0.0131	0.0129	0.0122
	3	0.0095	0.0199	0.0162	0.0144	0.0138
	Average	0.010	0.015	0.014	0.013	0.012
2.5NR-BC50	1	0.013	0.0136	0.0134	0.0127	0.0117
	2	0.014	0.0301	0.0285	0.0232	0.0208
	3	0.0147	0.0331	0.0303	0.0322	0.0297
	Average	0.014	0.026	0.024	0.023	0.021
5NR-BC50	1	0.0153	0.028	0.0273	0.0246	0.0214
	2	0.0196	0.0306	0.0293	0.0231	0.0223
	3	0.0154	0.0298	0.0274	0.0273	0.0268
	Average	0.017	0.029	0.028	0.025	0.024
7.5NR-BC50	1	0.0109	0.0161	0.016	0.0148	0.0143
	2	0.0129	0.0169	0.0161	0.0159	0.0152
	3	0.0131	0.0178	0.0157	0.0148	0.0147
	Average	0.012	0.017	0.016	0.015	0.015
10NR-BC50	1	0.0133	0.0201	0.0191	0.0161	0.016
	2	0.011	0.0172	0.0167	0.0163	0.0153
	3	0.0123	0.0198	0.018	0.0176	0.0159
	Average	0.012	0.019	0.018	0.017	0.016
0.5NR-BC60	1	0.0086	0.0165	0.0153	0.0148	0.0144
	2	0.0113	0.0147	0.013	0.0129	0.0125
	3	0.0112	0.0133	0.0127	0.0117	0.0116
	Average	0.010	0.015	0.014	0.013	0.013
1.5NR-BC60	1	0.0102	0.0174	0.0148	0.0135	0.0132
	2	0.0097	0.0139	0.0123	0.0114	0.0112
	3	0.0103	0.0128	0.0116	0.0112	0.0112
	Average	0.010	0.015	0.013	0.012	0.012

Table C. 3 The weight of dried specimen before swelling (W_0) and after immersion in toluene (W_t) of BC, NR and NR-BC60 and NR-BC70 films

samples	specimen	W_t (g)				
		Time (min)				
		W_0 (g) 0	30	60	120	240
2.5NR-BC60	1	0.0126	0.0276	0.0254	0.0247	0.0237
	2	0.0184	0.0293	0.0262	0.0258	0.0245
	3	0.0185	0.0302	0.0286	0.0252	0.0243
	Average	0.017	0.029	0.027	0.025	0.024
5NR-BC60	1	0.0103	0.0182	0.0173	0.0155	0.0146
	2	0.0089	0.0159	0.0142	0.0139	0.0132
	3	0.0098	0.0147	0.0133	0.0128	0.0126
	Average	0.010	0.016	0.015	0.014	0.013
7.5NR-BC60	1	0.0156	0.0212	0.0202	0.0196	0.0189
	2	0.014	0.0215	0.0213	0.018	0.0169
	3	0.0118	0.0206	0.0169	0.0164	0.0173
	Average	0.014	0.021	0.019	0.018	0.018
10NR-BC60	1	0.0194	0.0292	0.0272	0.0259	0.0247
	2	0.0188	0.0287	0.0275	0.0261	0.0254
	3	0.0167	0.0282	0.0263	0.0225	0.022
	Average	0.018	0.029	0.027	0.025	0.024
0.5NR-BC70	1	0.0081	0.0123	0.0112	0.0108	0.0104
	2	0.0089	0.0122	0.0118	0.0102	0.0102
	3	0.0094	0.0126	0.0105	0.0105	0.0105
	Average	0.009	0.012	0.011	0.011	0.010
1.5NR-BC70	1	0.0112	0.0141	0.0138	0.0118	0.0114
	2	0.0083	0.0128	0.0113	0.0109	0.0105
	3	0.0085	0.0137	0.0114	0.0109	0.0102
	Average	0.009	0.014	0.012	0.011	0.011
2.5NR-BC70	1	0.012	0.0234	0.0214	0.0191	0.0194
	2	0.0118	0.0191	0.0183	0.0179	0.0166
	3	0.0104	0.0182	0.0138	0.0133	0.0129
	Average	0.011	0.020	0.018	0.017	0.016
5NR-BC70	1	0.0163	0.0233	0.0217	0.0218	0.0202
	2	0.0136	0.0295	0.0238	0.0225	0.0223
	3	0.0143	0.0229	0.0212	0.0198	0.0188
	Average	0.015	0.025	0.022	0.021	0.020

Table C. 4 The weight of dried specimen before swelling (W_0) and after immersion in toluene (W_t) of BC, NR and NR-BC70 films

samples	specimen	W_t (g)				
		Time (min)				
		Wd (g) 0	30	60	120	240
7.5NR-BC70	1	0.011	0.0169	0.0157	0.0143	0.0138
	2	0.012	0.0186	0.0173	0.0169	0.0165
	3	0.012	0.0194	0.0169	0.0155	0.0147
	Average	0.012	0.018	0.017	0.016	0.015
10NR-BC70	1	0.0099	0.0157	0.0142	0.0139	0.013
	2	0.0114	0.0169	0.0155	0.0147	0.0145
	3	0.012	0.0184	0.0164	0.0143	0.0139
	Average	0.011	0.017	0.015	0.014	0.014

Table C. 5 Data for Figure 4.17

Time (min)	Toluene uptake (%)							
	NR-BC Concentration (%)							
	BC(0)	0.5	1.5	2.5	5	7.5	10	NR(100)
0	0.00	0.00	0.00	0.00	0.00	0.00	0.00	0.00
30	2.27	20.65	20.00	32.15	37.59	22.85	27.91	1858.73
60	8.71	19.43	18.28	24.78	26.55	16.89	23.58	2642.58
120	6.44	15.38	16.55	18.29	23.45	14.24	22.49	2122.62
240	6.44	10.53	13.79	13.86	21.72	9.60	19.24	1075.19

Table C. 6 Data for Figure 4.18

Time (min)	Toluene uptake (%)							
	NR-BC Concentration (%)							
	BC(0)	0.5	1.5	2.5	5	7.5	10	NR(100)
0	0.00	0.00	0.00	0.00	0.00	0.00	0.00	0.00
30	2.27	48.87	44.92	84.17	75.75	37.67	56.01	1858.73
60	8.71	33.12	33.11	73.14	67.00	29.54	46.99	2642.58
120	6.44	30.23	25.57	63.31	49.11	23.31	36.61	2122.62
240	6.44	24.12	20.98	49.16	40.16	19.78	28.96	1075.19

Table C. 7 Data for Figure 4.19

Time (min)	Toluene uptake (%)							
	NR-BC Concentration (%)							
	BC(0)	0.5	1.5	2.5	5	7.5	10	NR(100)
0	0.00	0.00	0.00	0.00	0.00	0.00	0.00	0.00
30	2.27	43.09	46.03	75.96	68.28	52.90	56.83	1858.73
60	8.71	31.83	28.15	62.02	54.48	41.06	47.54	2642.58
120	6.44	26.69	19.54	52.93	45.52	30.43	35.70	2122.62
240	6.44	23.79	17.88	46.46	39.31	28.26	31.33	1075.19

Table C. 8 Data for Figure 4.20

Time (min)	Toluene uptake (%)							
	NR-BC Concentration (%)							
	BC(0)	0.5	1.5	2.5	5	7.5	10	NR(100)
0	0.00	0.00	0.00	0.00	0.00	0.00	0.00	0.00
30	2.27	40.53	45.00	77.49	71.27	56.86	53.15	1858.73
60	8.71	26.89	30.36	56.43	50.90	42.57	38.44	2642.58
120	6.44	19.32	20.00	47.08	45.02	33.43	28.83	2122.62
240	6.44	17.80	14.64	42.98	38.69	28.57	24.32	1075.19

APPENDIX D. THE MECHANICAL PROPERTIES DATA.

1. Mechanical properties of NR-BC composite films prepared by immersion in NR suspension with the addition of ethanol.

Table D. 1 Young's modulus, tensile strength and elongation at break of 5 and 10% composite films immersion at 60°C.

Samples	Young's modulus (Mpa)		Tensile strength (Mpa)		Elongation at break (%)	
	Average[(a)]	SD	Average[(a)]	SD	Average[(a)]	SD
5.0NR-BC30	6881.67	1815.02	90.42	31.03	2.37	0.068
10.0NR-BC30	6677.67	1438.34	118.46	29.15	1.74	0.36

(SD: Standard deviation)

[(a)] Value are average of 3 specimens

2. Mechanical properties of NR-BC composite films prepared by immersion in NR suspension without the addition of ethanol.

Table D. 2 Data for Figure 4.37, 4.38 and 4.39

Samples	Young's modulus (Mpa)		Tensile strength (Mpa)		Elongation at break (%)	
	Average[(a)]	SD	Average[(a)]	SD	Average[(a)]	SD
BC	9135	778.63	111.63	4.53	0.65	0.062
NR	7.86	-	0.61	0.1	41.1	16.04
0.5NR-BC30	8516.25	841.46	130.17	10.57	1.6	0.138
1.5NR-BC30	6705.33	186.51	91.57	3.50	1.82	0.136
2.5NR-BC30	7376.00	101.72	204.7	2.86	2.37	0.217
5.0NR-BC30	7428.33	52.26	110.07	5.13	2.89	0.25
7.5NR-BC30	5650.67	45.76	64.77	14.66	1.77	0.39
10.0NR-BC30	3740.33	642.95	61.77	11.24	1.56	0.39
0.5NR-BC50	14577.00	205.38	222.73	39.1	2.13	0.17
1.5NR-BC50	13673.3	738.54	220.87	22.51	2.25	0.42
2.5NR-BC50	20051.3	69.14	392.43	3.74	3.25	0.2
5.0NR-BC50	11375.3	154.23	255.06	30.03	3.13	0.14
7.5NR-BC50	9201.67	466.19	146.36	13.98	2.55	0.54
10.0NR-BC50	8432	490.82	144.7	3.37	1.71	0.14
0.5NR-BC60	12389.33	1449.24	168.73	22.57	1.41	0.02
1.5NR-BC60	12389.67	40.34	190.23	15.05	1.62	0.15
2.5NR-BC60	15412.33	38.09	191.87	24.79	3.02	0.25
5.0NR-BC50	9490.67	630.34	227.33	13.97	3.59	0.3
7.5NR-BC60	3686.33	215.76	90.83	5.274	2.65	0.14
10.0NR-BC60	7812.33	1029.94	167.67	14.19	1.97	0.08
0.5NR-BC70	17544.7	300.83	215.27	5.04	1.9	0.21
1.5NR-BC70	16951.3	896.66	208.00	5.27	1.79	0.09
2.5NR-BC70	13869	1759.4	138.33	4.21	2.06	0.07
5.0NR-BC70	12648.3	963.35	183.80	16.01	1.95	0.04
7.5NR-BC70	6770.33	759.58	147.67	25.10	2.62	0.09
10.0NR-BC70	4085	107.56	42.91	11.40	0.81	0.19

(SD: Standard deviation)

[(a)] Value are average of 3 specimens

APPENDIX E. THE BIODEGRADABLE IN SOIL DATA.

Table E. 1 The temperature change for soil burial test.

Date / Month-year	Average daily temperature (℃)	Date / Month-year	Average daily temperature (℃)	Date / Month-year	Average daily temperature (℃)
April - 16		May - 16		May - 16	
24	37.7	1	36.8	16	33.4
25	39.1	2	37.4	17	29.8
26	37.6	3	35.8	18	34.5
27	37.8	4	36.8	19	33.4
28	36.6	5	33.6	20	35.8
29	34.8	6	35.5	21	35.8
30	36.5	7	34.8	22	37.5
		8	35.2	23	35.7
		9	36	24	36.5
		10	34.6	25	33.9
		11	35.4	26	32.8
		12	31.6	27	32.6
		13	33.6	28	32.3
		14	34.2		
		15	34.6		

VITA

Miss Kornkamol Potivara was born on April 15th, 1991 in Chanthaburi province, Thailand. She graduated in bachelor's degree in Textile Science and Technology, Faculty of Science, Thammasat University of Rangsit Campus, Pathum Thani province, Thailand in February 2013. She continued to study in Master's degree of Chemical Engineering, Department of Chemical Engineering, Faculty of Engineering, Chulalongkorn University in Bangkok, Thailand since 2014 and finished her study in April 2017.

Kornkamol Potivara and Muenduen Phisalaphong, "Development and characterization of Bacterial cellulose/natural rubber composite films" proceeding of the Pure and Applied Chemistry International Conference 2017 (PACCON2017), Centra Government Complex Hotel & Convention Centre Chaeng Watthana, Bangkok, Thailand, February 2-3, 2017